Delft University of Technology

Hydrogenation of carbon dioxide (CO_2) to fuels in microreactors
a review of set-ups and value-added chemicals production

Hafeez, Sanaa; Harkou, Eleana; Al-Salem, Sultan M.; Goula, Maria A.; Dimitratos, Nikolaos; Charisiou, Nikolaos D.; Villa, Alberto; Bansode, Atul; Leeke, Gary; More Authors

REVIEW

Check for updates

Hydrogenation of carbon dioxide (CO_2) to fuels in microreactors: a review of set-ups and value-added chemicals production

Sanaa Hafeez,[a] Eleana Harkou,[b] Sultan M. Al-Salem, [iD] [c] Maria A. Goula,[d] Nikolaos Dimitratos, [iD] [e] Nikolaos D. Charisiou,[d] Alberto Villa, [iD] [f] Atul Bansode,[g] Gary Leeke,[h] George Manos [iD] [a] and Achilleas Constantinou [iD] *[b]

Climate change, the greenhouse effect and fossil fuel extraction have gained a growing interest in research and industrial circles to provide alternative chemicals and fuel synthesis technologies. Carbon dioxide (CO_2) hydrogenation to value-added chemicals using hydrogen (H_2) from renewable power (solar, wind) offers a unique solution. From this aspect this review describes the various products, namely methane (C_1), methanol, ethanol, dimethyl ether (DME) and hydrocarbons (HC_s) originating *via* CO_2 hydrogenation reaction. In addition, conventional reactor units for the CO_2 hydrogenation process are explained, as well as different types of microreactors with key pathways to determine catalyst activity and selectivity of the value-added chemicals. Finally, limitations between conventional units and microreactors and future directions for CO_2 hydrogenation are detailed and discussed. The benefits of such set-ups in providing platforms that could be utilized in the future for major scale-up and industrial operation are also emphasized.

Introduction

Excessive extraction and utilization of fossil fuels combined with continuous greenhouse gas (GHG) emissions have led to increasing carbon dioxide (CO_2) concentration in the atmosphere.[1] Recently, 33 Gt per year of CO_2 emissions were recorded, which contributes to a rapid increase in atmospheric carbon levels from 280 ppm to 410 ppm (ref. 2) when compared with the preindustrial era. As a result of such conventional processes which utilise fossil fuels, the atmospheric CO_2 concentration is further predicted (Fig. 1) to increase to 570 ppm before the end of the century[3] if no CO_2

mitigation actions are taken. Two technologies, carbon capture and storage (CCS) and carbon capture and utilization (CCU), play a significant role in reducing CO_2 emissions.[4] Generating value added products through CO_2 hydrogenation utilising renewable hydrogen (H_2), produced by water electrolysis,[5] has proven to be a major challenge in order to seek alternative fuel synthesis routes.[6]

CCS is expected to play a vital role in limiting the GHGs emissions, as well as climate change attenuation in the future. Specifically, it is considered an attractive alternative for the decarbonisation of emissions from industries and can

[a] *Department of Chemical Engineering, University College London, London WC1E 7JE, UK*

[b] *Department of Chemical Engineering, Cyprus University of Technology, 57 Corner of Athinon and Anexartisias, 3036 Limassol, Cyprus.*
E-mail: a.konstantinou@cut.ac.cy

[c] *Environment & Life Sciences Research Centre, Kuwait Institute for Scientific Research, P.O. Box: 24885, Safat 13109, Kuwait*

[d] *Laboratory of Alternative Fuels and Environmental Catalysis (LAFEC), Department of Chemical Engineering, University of Western Macedonia, GR-50100, Greece*

[e] *Dipartimento di Chimica Industriale e dei Materiali, ALMA MATER STUDIORUM Università di Bologna, Viale Risorgimento 4, 40136 Bologna, Italy*

[f] *Dipartimento di Chimica, Università degli Studi di Milano, via Golgi, 20133 Milan, Italy*

[g] *Catalysis Engineering, Department of Chemical Engineering, Delft University of Technology, Van der Maasweg 9, 2629 HZ Delft, Netherlands*

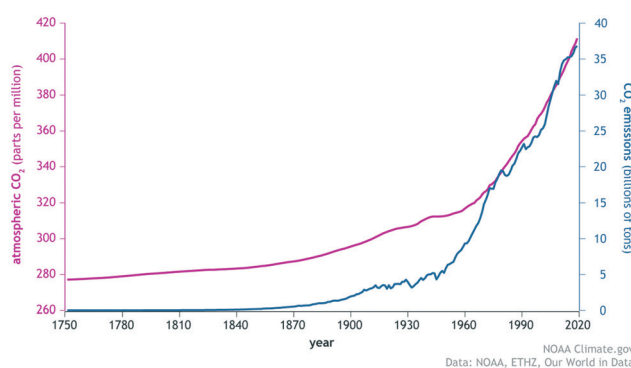[h] *School of Chemical Engineering, University of Birmingham, B15 2TT, UK*

Fig. 1 Schematic showing the amount of CO_2 in the atmosphere (purple line) has increased along with human emissions (blue line) since the start of the Industrial Revolution in 1750.[7]

This journal is © The Royal Society of Chemistry 2022

React. Chem. Eng., 2022, 7, 795–812 | **795**

also be merged with low carbon or carbon neutral bioenergy to produce negative emissions.[1] Whereas CCU attempts both the reduction of CO_2 emissions in the atmosphere and the substitution of conventional raw materials in distinct types of industrial processes through CO_2 hydrogenation. This method focuses on using carbon free viable technologies.[8] Renewable H_2 is generated through water electrolysis by applying electricity from renewable sources such as solar and wind and is widely used for the CO_2 hydrogenation processes.[9]

There are several carbon utilisation methods. CO_2 can be used as a feedstock for the production of fuels and chemicals. The main products derived from CO_2 are formic acid, urea, methanol, salicylic acid and cyclic carbonates. CO_2 if often converted into fuels or chemicals through biochemical, electrochemical, photochemical, thermo-catalytic, and hybrid methods. Industrial carbon emissions can be efficiently used *via* mineralisation processes to produce a range of products. The reaction is thermodynamically favourable, and a range of feedstocks (*e.g.*, alkaline solid wastes and natural silicate ores) can be applied for the mineralisation processes. The mineralisation process can be divided into four main categories: direct and indirect carbonation, carbonation curing and electrochemical mineralisation.[10]

Potential of both conventional reactor units and microreactors in CO_2 hydrogenation has been demonstrated to obtain the chemical fuels. Conventional units such as continuously stirred tank reactors, fixed-bed reactors, fluidised-bed reactors (FBRs), packed-bed reactors and slurry reactors, have broadly been operational at industrial scale for the synthesis of value chemical fuels such as methane, methanol, ethanol, DME and higher hydrocarbons,[11] due to low cost and high heat and mass transfer.[12] Regardless of their applications, conventional units represent a high pressure drop, complex hydrodynamics and modelling.[11,13]

The CO_2 hydrogenation process into hydrocarbons can be classified as two groups. This is the methanation reaction and the production of hydrocarbons through the Fischer–Tropsch (FT) process.[14] Consequently, CO_2 can be hydrogenated to methane (CH_4), methanol (CH_3OH), ethanol (C_2H_5OH), lower olefins, dimethyl ether (DME) and higher hydrocarbons.[15,16] A scheme of the main products of CO_2 hydrogenation can be seen in Fig. 2. The production of olefins, *i.e.*, ethylene and propylene, from the hydrogenation of CO_2 is a significant route. These olefins are the two most widely produced petrochemicals in the world. The worldwide ethylene and propylene consumption was nearly 150 million and 100 million metric tons, respectively. The demand for these chemicals signifies their imperative use in the chemical process industries as feedstocks and other materials, to produce solvents, plastics, polymers and cosmetics. Moreover, olefins can be further upgraded into long-chain hydrocarbons for use as fuels, rendering them as a high potential for using up to 23% of carbon emissions.[17] Generation of these chemical fuels was initially based on
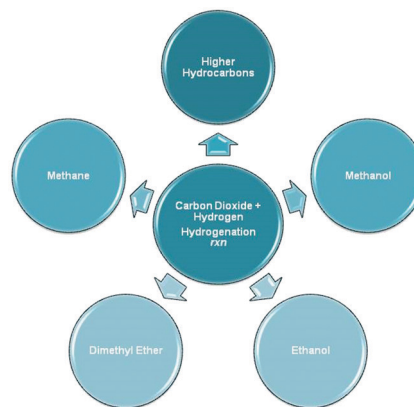

Fig. 2 Schematic representation of carbon dioxide hydrogenation to value-added chemical fuels.

conventional reactor processes. However, many studies now are focused on the production of these fuels using microreactors, due to their potential in accelerating the generation of these value-added fuels.[18]

Great efforts have recently been accomplished to prepare microreactors with the aim of producing chemical fuels through CO_2 hydrogenation.[19] Microreactors such as continuous flow microreactors,[20,21] micro packed-bed reactors,[22,23] membrane,[24,25] and microplasma reactors can be used to enhance various unit operations and reactions in micro space. Moreover, microreactors exhibit pivotal advancements in chemical engineering, leading to excellent output yield of chemical fuels.[26] Microreactors present high heat and mass transfer for highly exothermic reactions, while the dimensions of the microreactors components promote the enhancement of construction and operation.[19,27] Finally, the microscale volume capacity of microreactors have also provided efficient progress of continuous flow reactions since they considerably decrease the quantity of materials required to improve reaction conditions.[28] These reactors were used to synthesise chemical fuels for energy demand.

This review will provide a succinct illustration of the different routes performed to produce synthetic gases through CO_2 hydrogenation according to the challenges faced by conventional units and microreactors. The contribution of conventional units during CO_2 hydrogenation process will then be described. In addition, microreactors used to produce synthetic gases will be explained. Finally, limitations between conventional units and microreactors as well as future directions will be highlighted and discussed.

CO_2 hydrogenation to value added chemicals synthesis routes

Hydrogen can be produced using various processes, Fig. 3 shows a brief overview of the many ways hydrogen can be obtained. Hydrogen required to react with CO_2 is conventionally produced from the steam reforming of non-

796 | *React. Chem. Eng.*, 2022, **7**, 795–812

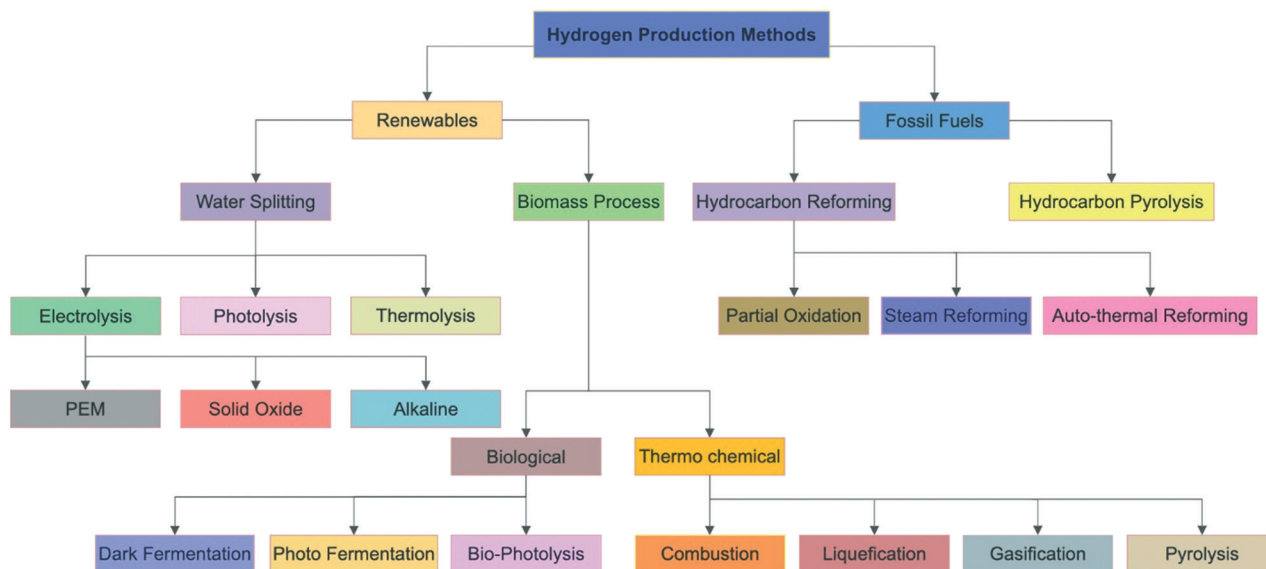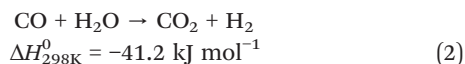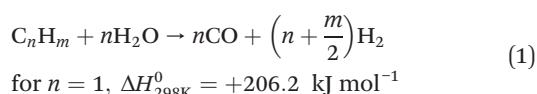This journal is © The Royal Society of Chemistry 2022

Fig. 3 Overview of hydrogen production routes.

renewable hydrocarbon feedstocks, and this been the preferred industrial method for several decades.

Typically, the steam reforming process occurs *via* two reactions: (1) the steam reforming of the hydrocarbons, and (2) the water gas shift (WGS) reaction.[29]

$$C_nH_m + nH_2O \rightarrow nCO + \left(n + \frac{m}{2}\right)H_2$$
$$\text{for } n = 1, \ \Delta H^0_{298K} = +206.2 \ \text{kJ mol}^{-1} \tag{1}$$

$$CO + H_2O \rightarrow CO_2 + H_2$$
$$\Delta H^0_{298K} = -41.2 \ \text{kJ mol}^{-1} \tag{2}$$

Another conventional method for hydrogen production is autothermal reforming. This process is like the previously described steam reforming; however, a proportion of the fuel reacts with oxygen to produce the thermal energy required in the reforming reaction which is an endothermic process. The generalised reaction for the autothermal reforming can be expressed as:[30]
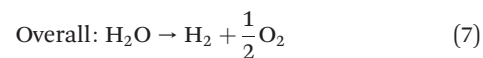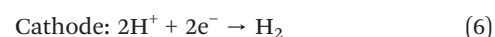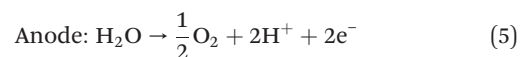
$$C_nH_mO_p + xO_2 + (2n - 2x - p)H_2O \rightarrow nCO_2$$
$$+ \left(\frac{m}{2} + 2n - 2x - p\right)H_2 \tag{3}$$
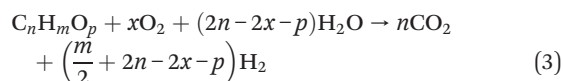
The value of x is related to the composition of the hydrocarbon.

The gasification of coal is another significant reaction for the industrial production of hydrogen. The reaction products consist of syngas (CO and H_2), and the CO can be further upgraded to H_2 and CO_2 *via* the WGS reaction. The primary reaction can be given by:[31]

$$C_nH_m(\text{coal}) + nH_2O \rightarrow nCO + \left(n + \frac{m}{2}\right)H_2 \tag{4}$$

Nonetheless, the coal gasification reaction is highly endothermic and requires reaction temperatures of 1273 K to acquire the desired product yield. On the other hand, the WGS reaction is exothermic and so lower reaction temperatures for the CO conversion are needed.[31] Typically, the coal gasification reaction is performed in a reactor with a temperature of 1273 K. The syngas product is then fed to another reactor which has a temperature below 673 K for the conversion of CO.[32]

The other approach is to produce the hydrogen from renewable energy sources. The electrolysis of water is one of the well-established methods to produce hydrogen as it utilises renewable and generates solely pure oxygen as a by-product. Furthermore, the electrolysis process is envisioned to use power from sustainable energy sources, such as wind, solar and biomass. However, currently, only 4% of the total hydrogen produced is coming from the electrolysis of water. This is mainly due to the economic issues.[33] The various electrolytes systems for the electrolysis of water can be represented by alkaline water electrolysis (AWE), proton exchange membranes (PEM), alkaline anion exchange membranes (AEMs), and solid oxide water electrolysis (SOE). The water electrolysis process can be represented by the following:[34]

$$\text{Anode: } H_2O \rightarrow \frac{1}{2}O_2 + 2H^+ + 2e^- \tag{5}$$

$$\text{Cathode: } 2H^+ + 2e^- \rightarrow H_2 \tag{6}$$

$$\text{Overall: } H_2O \rightarrow H_2 + \frac{1}{2}O_2 \tag{7}$$

The photocatalytic splitting of water with TiO_2 powders is the most basic configuration of the process, which is comprised

This journal is © The Royal Society of Chemistry 2022

React. Chem. Eng., 2022, **7**, 795–812 | 797

of a sole type of semiconductor particles in continuous contact with water. Once excited by an incident photon with a greater energy than the bandgap of the semiconductor, an electron in the valence band can be pushed to the conduction band and generates a hole. Subsequently, the hole and electron separate specially and diffuse to the surface of the semiconductor to take part in the hydrogen evolution reaction and oxygen evolution reaction.[35]

The hydrogenation process aids the reduction of atmospheric CO_2 while producing fuels and value-added chemicals.[36] CO_2 hydrogenation to value added chemical fuels is considered a beneficial process, provided that renewable H_2 is supplied.[37,38] H_2 is a major utility that is typically produced from conventional petroleum reforming and could has major environmental implications. Remarkable advancements have been accomplished in the synthesis of CH_4 (C_1), methanol (CH_3OH), ethanol (C_2H_6O), dimethyl ether (DME) and higher hydrocarbons (HCs) directly from CO_2 hydrogenation. Mixture of CO_2/H_2 is required for the conversion into value added chemical fuels through the Fischer–Tropsch process and is often utilised widely in industry. Finally, synthesis of alcohols is more demanding than hydrocarbons by reason of accurate control of C–C coupling.[39] The resulting products of CO_2 hydrogenation, such as hydrocarbons and methanol, are excellent alternative fuels for internal combustion engine with ease in storage and transportation. This alleviates many of the challenges associated with the use of fossil fuels.[36] Table 1 provides a summary of the main catalysts which are applied for the hydrogenation of CO_2 into fuels and chemicals.

There are some issues which exist for the conversion of CO_2 into value-added chemicals. Although the noble metal catalysts have a good performance, they are highly costly, and lack of availability limits their wide scale applications for the hydrogenation of CO_2 to methane and ethanol. An alternative to this would be other metal catalysts, such as Ni; however, these catalysts are highly susceptible to deactivation due to sintering and carbon poisoning.[40] A similar issue exists with the $Cu/ZnO/Al_2O_3$ catalyst used for the hydrogenation of CO_2 to methanol. A problem faced with this catalyst is the low selectivity towards methanol caused by the reverse water gas shift (RWGS) reaction. Furthermore, the catalyst activity declines rapidly due to the water product, which leads to the sintering of the Cu component during the reaction.[41] The typical catalysts used for ethanol synthesis can suffer from the effects of high temperature, which promote the RWGS pathway and aids the production of undesirable CO.[42]

Similarly, a prominent issue with the conversion of CO_2 to higher hydrocarbons is the high selectivity towards methane and light saturated hydrocarbons.[43]

CO_2 to methane

Methane (C_1) is regarded a principal constituent of natural gases and can be successfully utilised in industry, energy and transportation sectors.[44,45] The production of methane through CO_2 hydrogenation is the most sustainable and convenient pathway to store significant quantities of energy generated from renewable sources.[46–54] CO_2 hydrogenation to C_1 reaction, initially revealed by the French chemist Paul Sabatier,[1,55] can be represented as:[56,57]

$$CO_2 + 4H_2 \rightleftharpoons CH_4 + 2H_2O$$
$$\Delta H_{298K} = -165 \text{ kJ mol}^{-1} \quad (8)$$
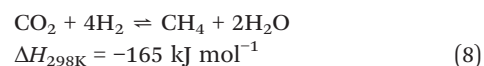
CO_2 to methanol

Methanol is reported as one of the dominant chemical raw materials in the chemical and petrochemical industry through which methyl methacrylate, dimethyl carbonate, chloromethane, acetic acid, formaldehyde, methylamines, dimethyl terephthalate and methyl tertiary butyl ether are generated.[6] Methanol synthesis through CO_2 hydrogenation has attracted tremendous interest as noble and oxide-supported metals have been regarded promising catalysts in controlling both the activity and selectivity of methanol.[60,83–91] Direct methanol (CH_3OH) generation through CO_2 hydrogenation is represented as:[92,93]

$$CO_2 + 3H_2 \rightleftharpoons CH_3OH + H_2O$$
$$\Delta H_{298K} = -41.1 \text{ kJ mol}^{-1} \quad (9)$$
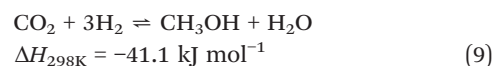
Remarkable progress has been made in CO_2 hydrogenation to methanol and specifically in developing Cu and In-based catalysts.[94] It is reported that over a $Cu–ZnO–Al_2O_3$ catalyst, high CH_3OH selectivity up to 98.2% can be accomplished under conditions of P = 36 MPa and T = 220–300 °C (ref. 95) and a In_2O_3/ZrO_2 catalyst CH_3OH selectivity can be up to 99.8% under conditions of P = 5 MPa and T = 300 °C.[96] The remarkable selectivity and conversion are due to the exceedingly high-pressure conditions used for the study. Considering the catalytic kinetics for methanol synthesis, development of highly effective noble metal-based catalysts in terms of selectivity and stability is demanded.[97] Hartadi

Table 1 Summary of catalysts applied for the conversion of CO_2 into value-added chemicals

Process route	Catalytic system
Methane	Ru,[50,58,59] Rh,[60,61] Pd,[62] Ni,[53,63] and Co (ref. 40 and 64)
Methanol	$Cu/ZnO/Al_2O_3$[60,65,66]
Ethanol	Ru,[67] Pt,[68] Co,[69] Fe (ref. 70) and Cu (ref. 71 and 72)
DME	Cu-based,[73–75] solid acid catalyst[76,77] and zeolites[78,79]
Higher hydrocarbons	Fe (ref. 80–82)

798 | *React. Chem. Eng.*, 2022, **7**, 795–812

This journal is © The Royal Society of Chemistry 2022

et al.[98] reported that over an Au-based catalyst supported by TiO_2, ZrO_2, ZnO and Al_2O_3, high CH_3OH selectivity up to 82% (ref. 97) is accomplished under conditions of P = 5 bar and T = 220–240 °C. Malik *et al.*[99] have concluded that over PdZn/CeO_2 and Ca-doped PdZn/CeO_2 catalysts, high CH_3OH selectivity of up to 100% is achieved under conditions of P = 30 bar and T = 220 °C.

Lee *et al.*[49] performed a techno-economic analysis for the hydrogenation of CO_2, and methane, to methanol. Two processes were developed to investigate the production of methanol from landfill gas. The first was a stand-alone process (L2M-SA), and the second process had a hydrogen supply (L2M-HS). The results from the techno-economic analysis showed that the L2M-HS process has poorer economics, as opposed to the stand-alone process, due to the excessive cost of the hydrogen supply. Furthermore, the unit production cost (UPS) of the L2M-HS process was found to be around 12% higher than the L2M-SA process. Nonetheless, the methanol produced from the L2M-HS process can be economically viable with the actual methanol market if cheaper hydrogen supply routes are available, *e.g.*, using hydrogen which has been produces as a by-product from industry. The study concluded that the UPC of methanol is approximately 392–440 $ per tonne, which is competitive with other conventional methanol production processes. Furthermore, the lower environmental emissions with the current process make it an environmentally clean approach.

CO_2 to ethanol

The conversion of CO_2 hydrogenation to high alcohols remains an exceptional challenge due to the understanding of parallel and successive reactions. Noble metals such as Au, Pt and Pd are reported as catalysts for direct production of ethanol from CO_2 hydrogenation with high selectivity up to 88.1% over a Pt/CO_3O_4 catalyst under conditions of P = 8 MPa and T = 220 °C. Recent studies have shown that non-noble and metal-based catalysts are investigated to provide highly efficient liquid phase ethanol from CO_2 hydrogenation.[39,69,71,100–106] Direct CO_2 hydrogenation to ethanol is represented below:[107]

$$2CO_2 + 6H_2 \rightleftharpoons C_2O_5OH + 3H_2O$$
$$\Delta H_{298K} = -86.7 \text{ kJ mol}^{-1} \tag{10}$$
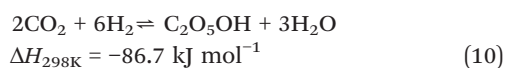
CO_2 to DME

DME is regarded as a significant chemical intermediate for the generation of various chemicals such as diethyl sulphate, methyl acetate, light olefines, and gasoline.[108] The hydrogenation of CO_2 to DME has attracted great interest with several heterogeneous catalysts.[74,75,77,78,109–112] Direct CO_2 hydrogenation to DME is shown below:

$$CO_2 + 6H_2 \rightleftharpoons CH_3OCH_3 + 3H_2O$$
$$\Delta H = -122.2 \text{ kJ mol}^{-1} \tag{11}$$
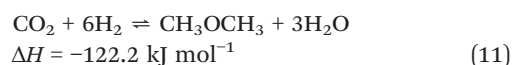
Cu–ZnO–Al_2O_3 catalysts and a mesoporous HZSM-5 zeolite are used in DME synthesis, providing great resistance and improving the mass transfer process during the reactions.[113] Alvarez *et al.*[114] reported that direct CO_2 hydrogenation to DME requires a bifunctional catalyst in order to perform methanol synthesis and methanol dehydration. Utilisation of γ-Al_2O_3 and H-ZMS-5 catalysts[115] is investigated for direct conversion of synthetic gas (syngas) to DME. Methanol synthesis can be a physical mixture containing a methanol synthesis catalyst and a solid catalyst which are mixed, and the function of the reactions are divided. Methanol dehydration is considered an integrated mixture where the catalytically active products of the reactions are located to the nearest position so as to ease DME synthesis.[114] Tokay *et al.*[116] investigated that over an Al@SBA-15 and mesoporous $AlSi_3$ catalyst, high DME selectivity of up to 100% is achieved under condition of T = 300–400 °C and a space time of 0.0027 s g cm^{-3}.
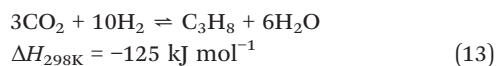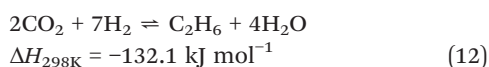
Michailos *et al.*[117] investigated the production of DME from the captured CO_2 hydrogenation within the context of power-to-liquid context. The calculations were based upon a plant which generates approximately 740 tonnes per day of DME. The results from the economic analysis revealed that net production cost of DME was 2112 € per tonne, and the minimum DME selling price (MDSP) was 2193 € per tonne. The latter value is 5 times greater than the average gate price of conventional diesel in 2016. This high cost is mainly related to electricity price, due to the electrolysis unit, as opposed to the parameters related to the CO_2 capture and conversion plants. A subsidised or free of charge electricity supply will make the DME price more competitive; although, this will be unlikely due to the establishment of other technological options.

CO_2 to higher hydrocarbons

Higher hydrocarbons, such as light olefins and particularly ethylene and propylene generation, has gained great interest in the petrochemical industry.[118] Direct CO_2 hydrogenation to higher hydrocarbons is described as the combination of conversion CO_2 through the FT process and reverse water gas shift (RWGS) reaction.

The typical catalysts applied for the process are Fe-based due to their ability to catalyse both reactions. They can be utilised in bulk form or as supported iron oxides. In order to diminish the selectivity towards methane, the catalysts are doped with oxides of Cu, K, Mn, and/or Ce.[119] The most encouraging catalysts for this process are K promoted Fe/Al_2O_3 catalysts with K contents of up to 0.5 mol-K mol^{-1} of Fe. Nonetheless, these catalysts experience low efficiencies for the hydrogenation of CO_2. This remains a major challenge for the production of higher hydrocarbons.[120] Recent studies have proven that CO_2 hydrogenation to value added chemical fuels can be realised by using the main catalysts for CO_2 hydrogenation with zeolites.[19]

This journal is © The Royal Society of Chemistry 2022

React. Chem. Eng., 2022, **7**, 795–812 | **799**

CO$_2$ hydrogenation to higher hydrocarbons can be described below:

$$2CO_2 + 7H_2 \rightleftharpoons C_2H_6 + 4H_2O$$
$$\Delta H_{298K} = -132.1 \text{ kJ mol}^{-1} \quad (12)$$

$$3CO_2 + 10H_2 \rightleftharpoons C_3H_8 + 6H_2O$$
$$\Delta H_{298K} = -125 \text{ kJ mol}^{-1} \quad (13)$$

Conventional reactors in CO$_2$ hydrogenation

The most used conventional reactors for the hydrogenation of CO$_2$ are continuously stirred tank reactors (CSTRs), fluidised bed reactors (FBRs) and fixed bed reactors. Fig. 4 shows a schematic of these conventional reactors.
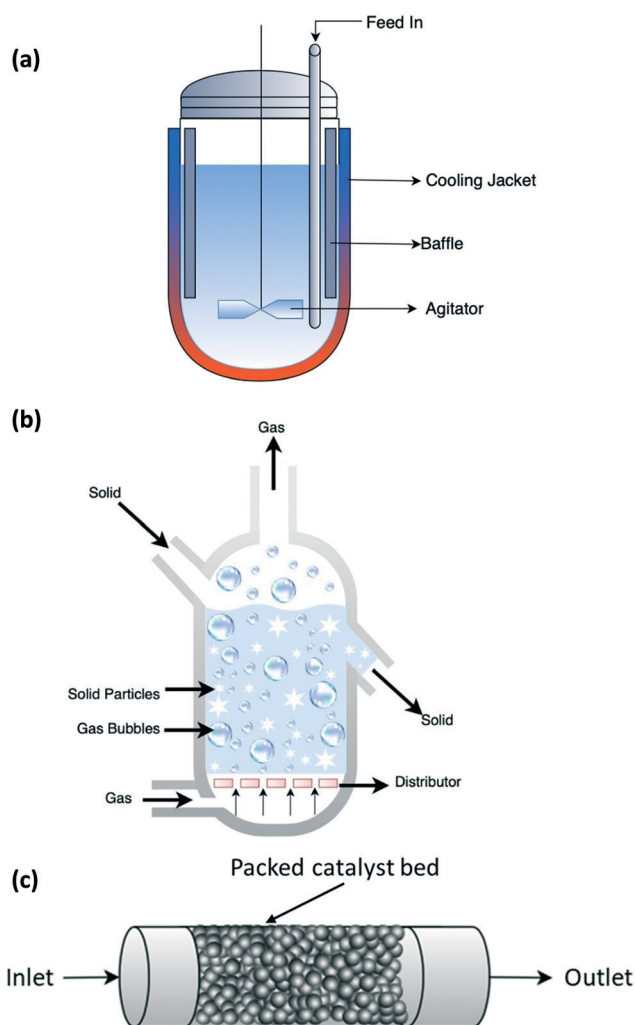

Fig. 4 Schematic representation of the conventional reactors used commonly for the hydrogenation of CO$_2$. (a) CSTR; (b) FBR; and (c) fixed bed reactor.

Continuously stirred tank reactor (CSTR)

CSTRs are considered as the most conventional reactors in the field of CO$_2$ hydrogenation. One of the operational issues with CSTRs is complex non-linear behaviour. These characteristics depict the requirement of a complex control system design. The results obtained from this non-linear analysis are significant as it allows the determination of difficult operating points, in order to remove them. As an example, it may be useful to operate around an unstable operating point, which can result in observation of higher product yields.[121] Nonetheless, CSTRs can provide wide operating range, as they can operate under steady state with continuous flow of both reactants and products.[122] Fig. 5 shows a schematic of the CSTR process of the hydrogenation of CO$_2$ to produce methane. Chiavassa et al.[123] employed a Berty-type CSTR reactor for methanol synthesis through CO$_2$/H$_2$ over Ga$_2$O$_3$–Pd/SiO$_2$ catalysts. The results showed that under conditions of P = 1–4 MPa and T = 508–523 K, CO$_2$ conversion to CH$_3$OH was up to 70% and selectivity of CH$_3$-OH up to 50–55% was achieved.

Dorner et al.[124] used a CSTR for C$_1$ and C$_2$–C$_5$ higher hydrocarbons synthesis, using Mn/Fe and K/Mn/Fe catalysts. Hydrogenation of CO$_2$ was accomplished under conditions of P = 13.6 atm, T = 563 K and gas hourly space velocity (GHSV) of 0.015 L g^{-1} s^{-1}. The results showed that over Mn/Fe and K/Mn/Fe catalysts, CO$_2$ conversion to methane was up to 34.4% and 41.4% and selectivity was up to 42% and 29.4%, respectively. In addition, for higher hydrocarbons synthesis, the results showed that over Mn/Fe and K/Mn/Fe catalysts, CO$_2$ conversion to C$_2$–C$_5$ higher hydrocarbons was up to 41.4% and 37.7%, and the selectivity reached 62.4% and 55.3%, respectively.

Lefebvre et al.[125] used a CSTR reactor to identify the study on the three-phase CO$_2$ methanation reaction, applying a commercial Ni/SiO$_2$ catalyst, suspended in the liquid phase. Feed gases were heated in a preferred temperature between 220 °C and 320 °C and mixed in a tempered feed tank. The results showed that under conditions of P = 1 atm and T = 220–320 °C, CO$_2$ conversion to methane could not increase any further for an agitator speed above ca. 1000 L min^{-1} and CH$_4$ selectivity during the process was up to 95%.

Kirchbacher et al.[126] also used a CSTR reactor to produce CH$_4$ derived from the reaction of CO$_2$ and renewable H$_2$, generated by water electrolysis. For methane synthesis through CO$_2$ hydrogenation, two main processes were achieved. Initially, a high H$_2$/CO$_2$ ratio was applied to prevent thermal effects of the spherical catalyst Meth 134®, which provides a high CO$_2$ conversion to CH$_4$ that is approximately 80%. Methanation process was conducted at three pressure levels of 6, 10, 14 bar and a GHSV of 3.000, 4.000, 5.000 and 6.000 h^{-1} under conditions of T = 395–425 °C. Secondly, under semi-lab conditions biogas and synthetic H$_2$ were employed to generate methane. The feed gas composition was investigated by five pressure levels of 6, 8, 10, 12 and 14 bar. However, GHSV was limited to 4.000 h^{-1}. Methane
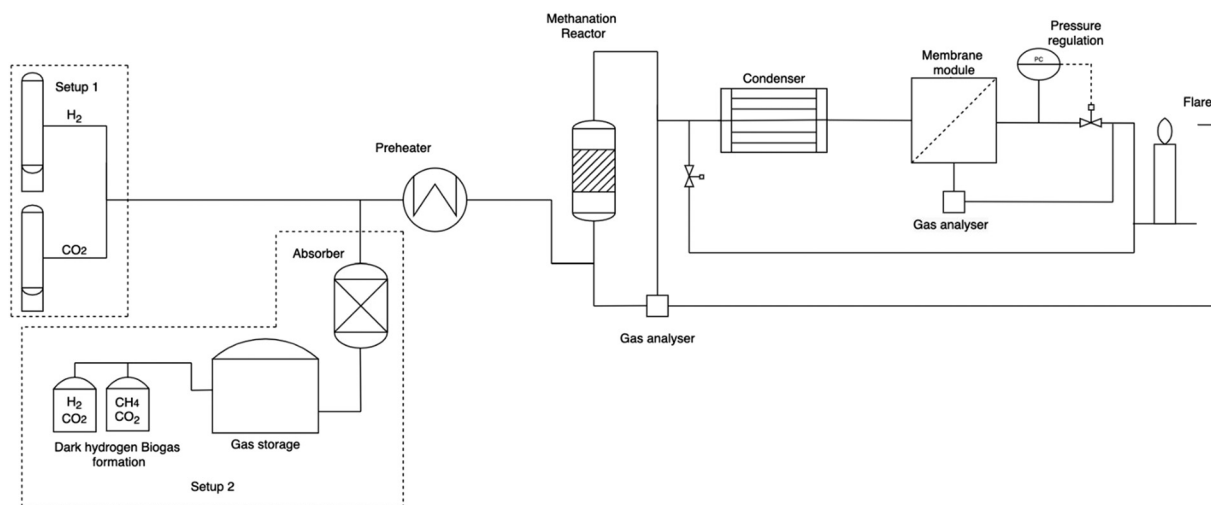
800 | React. Chem. Eng., 2022, **7**, 795–812

This journal is © The Royal Society of Chemistry 2022

Fig. 5 Flow sheet of the connected processes for CO_2 hydrogenation to methane using a CSTR.

productivity reached a level of 85% v/v under condition of $P = 14$ bar.

García-Trenco et al.[127] used a CSTR reactor to generate methanol through CO_2 hydrogenation, applying bimetallic Pd–In nanoparticles as catalysts. The results showed that Pd/In catalysts reduced methanol activity up to 50%, whereas the catalyst including Pd/In intermetallic nanoparticles (NPs) exhibited high CH_3OH rate up to 70% and high CH_3OH selectivity up to 90%. Furthermore, the optimum PdIn-based catalyst displayed an improvement in stability-the methanol production rate decreased by 20% after 120 h run, compared with 30% for the $Cu/ZnO/Al_2O_3$ catalyst (after 25 h).

A further study performed by García-Trenco et al.[128] investigated the hydrogenation of CO_2 to methanol using colloidal Pd_2Ga-based catalysts in a CSTR reactor. The colloidal Pd_2Ga-based catalysts shown 2-fold higher intrinsic activity than commercial $Cu–ZnO–Al_2O_3$ (60.3 and 37.2 × 10^{-9} mol_{MeOH} m^{-2} s^{-1}) and 4-fold higher on a Cu or Pd molar basis (3330 and 910 μmol $mmol_{Pd\ or\ Cu}^{-1}$ h^{-1}) in liquid phase at a reaction pressure of 50 bar. The results showed a good correlation between the intrinsic activity and the content of Ga_2O_3 surrounding the Pd_2Ga nanoparticles (XPS), indicating that methanol is produced via a bifunctional mechanism concerning both phases. A steady decrease in methanol selectivity (60 to 40%) was observed when temperature was raised (190–240 °C) whilst an optimum methanol production rate was observed at 210 °C. Nonetheless, when compared to the conventional $Cu–ZnO–Al_2O_3$, which suffered from around a 50% loss of activity over 25 h time on stream, the Pd_2Ga-based catalysts sustained activity over this time frame.

In industry, it is common to utilise multifunctional metallic copper and zinc oxide catalyst on alumina (CZA). Huš et al.[129] investigated experimentally, and via multiscale modelling, of commercial-like catalyst (Zn_3O_3/Cu) and three other Cu/metal oxide combinations (Cr_3O_3/Cu, Fe_3O_3/Cu, and Mg_3O_3/Cu), synthesised by co-precipitation. The results showed that the formate species pathway (HCOO → H_2COO

→ H_2COOH → H_2CO → H_3CO) dominates on the studied Cu-based catalysts. Although, Zn_3O_3/Cu exhibited the highest conversion and a moderate CH_3OH product selectivity, the former was smaller for Mg_3O_3/Cu. Furthermore, Cr_3O_3/Cu was ideal in terms of yield, but with exceptionally low CH_3OH productivity, whereas Fe_3O_3/Cu functioned poorly overall.

Fluidised bed reactors (FBRs)

FBRs can be used for multiphase reactions due to the higher heat and mass transfer and the efficient mixing among reactants. Furthermore, FBRs are regarded as excellent in terms of CO_2 hydrogenation to value chemical fuels, conversion of syngas, selectivity and economic feasibility.[4] Kim et al.[130] used a FBR for direct hydrocarbon synthesis through CO_2 hydrogenation over K-promoted iron catalysts. A bench-scale fluidised bed (inner diameter of 0.024 m and length of 0.6 m) was applied for hydrocarbons synthesis. The results showed that under conditions of pressure between 1 and 2.5 MPa and temperature of 300 °C, CO_2 conversion to olefins was up to 46.8%, and olefins selectivity up to 89.3% was accomplished.
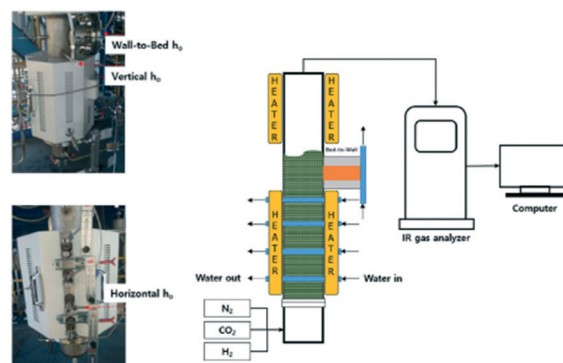

Fig. 6 Bench scale fluidised bed reactor (left) and schematic diagram (right)[131] (copyright permission obtained from Elsevier).

This journal is © The Royal Society of Chemistry 2022

React. Chem. Eng., 2022, **7**, 795–812 | **801**

Nam *et al.*[131] used a bench-scale bubbling fluidised bed reactor (shown in Fig. 6) for CO_2 hydrogenation to methane by applying a Ni-based catalyst. Ni as a fluidising component and active catalytic constituent was selected for use into a bubbling fluidised bed reactor for CO_2 hydrogenation to methane. The bubbling fluidised reactor (diameter of 0.14 m and height of 2 m) was encircled by an electrical heater. The results showed that a high CO_2 conversion to CH_4 up to 98% and CH_4 purity up to 81.6% was achieved, under conditions of temperature between 280 °C and 300 °C and heat transfer (h_o) of 115 W m^{-2}.

Jia *et al.*[132] employed a fluidised bed reactor for direct CO_2 hydrogenation to methane, applied a Ni–Co based catalyst supported on TiO_2-coated SiO_2 spheres. A bench-scale fluidised bed reactor was utilised for CO_2 methanation, consisted of a quartz tube which was positioned in a tubular electric furnace (inner diameter of 22 mm and length of 1 m). The results showed that under conditions of ambient pressure and temperature of 260 °C for over 120 h, CO_2 conversion to methane was up to 52%, and CH_4 selectivity up to 97% was achieved.

Fixed bed reactors

Fixed bed reactors are the most common type of reactor, consisting of solid catalysts particles which are loaded and packed in the bed.[133] In fixed bed reactors, gas, and liquid flow below the catalyst bed from the top of the reactor to the bottom, without stirring. Furthermore, CO_2 and H_2 are in direct contact with the catalyst particles.[134] One of the major points in fixed bed reactors is the temperature control in exothermic reactions. The desired minimal CO_2 conversion can reach 90%. Finally, the reaction time varies with the catalyst due to the generation of H_2O and the reaction rates.[135]

Ducamp *et al.*[136] used a cylindrical annular fixed bed reactor (inner diameter of 20 mm, outer diameter of 50 mm and length of 34 mm) to produce methane, by applying a commercial catalyst made of a Ni active phase scattered on alumina trilobe extrudates, and to analyse CO_2 and C_2H_6. The results showed that under reaction conditions of pressure from 0.4 to 0.8 MPa and a temperature between 200 °C and 275 °C, CO_2 conversion to CH_4 was up to 85% and 89%, respectively.

Jaffar *et al.*[137] used a fixed bed reactor containing a gas preheater to generate methane using a 10% wt Ni–Al_2O_3 catalyst. The results showed that under condition of temperature 360 °C methane yield up to 57.6% and methane selectivity up to 98% was achieved. Kiewidt *et al.*[138] used a fixed bed reactor to produce methane. A 5% wt Ru-based catalyst supported by ZrO_2 loaded directly in the reactor with diluted catalyst powder. The results showed that under reaction conditions of pressure 10 bar and temperature 300 °C, methane yield up to 90% was generated.

Castellani *et al.*[139] used a stainless mono tubular fixed bed reactor CO_2 methanation. The results showed that under
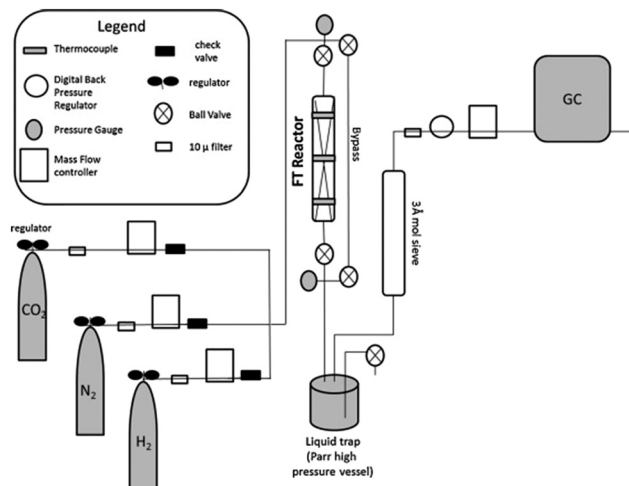

Fig. 7 Flow sheet for CO_2 hydrogenation using a fixed bed reactor[134] (copyright permission obtained from Elsevier).

reaction conditions of pressure from 2 to 20 bar and temperature between 250 °C and 400 °C, methane conversion of 31.36%, methane content up to 97.24% and CO_2 conversion up to 99.6% was achieved. Willauer *et al.*[134] employed a fixed bed reactor (shown in Fig. 7) (stainless steel tube) for direct synthesis of hydrocarbons through CO_2 hydrogenation, using a γ-Al_2O_3 supported modified iron-based catalysts. The results showed that under conditions of P = 265 psig and T = 300 °C, CO_2 conversion of C_2–C_5 hydrocarbons was up to 41.4% and selectivity was up to 62.4%.

Pastor-Pérez *et al.*[140] used a fixed bed reactor for direct CO_2 hydrogenation to methane and applied Ni/CeO_2–ZrO_2 catalysts promoted with Mn and Co. CO_2 methanation process was conducted in a vertical continuous fixed bed quartz reactor (inner diameter of 10 mm), using 250 mg of the catalyst. The results showed that under conditions of T = 400 °C, CO_2 conversion to CH_4 up to 70% and CH_4 selectivity up to 99% was achieved. Furthermore, Bradley *et al.*[141] employed a fixed bed reactor to identify the role of the catalyst environment on CO_2 hydrogenation by applying a Macrolite® supported iron-based catalysts. The results showed that under conditions of T = 280–320 °C, CO_2 conversion to methane and C_2–C_5 higher hydrocarbons up to 22–36%, CH_4 selectivity up to 26% and C_2–C_5 higher hydrocarbons selectivity up to 60–69% were achieved.

Zhang *et al.*[142] investigated the selective hydrogenation of CO_2 and CO into olefins over sodium- and zinc-promoted iron carbide catalysts in a fixed bed reactor. The results showed that the selectivity of C_2–C_{12} olefins reached 78%, and the space–time yield of olefins attained as high as 3.4 g g_{cat}^{-1} h^{-1} in CO_2 hydrogenation. Furthermore, the intrinsic formation rate of C_2–C_{12} olefins in CO hydrogenation was approximately twice higher when compared to that in CO_2 hydrogenation. The hydrogenation of CO_2 to olefins proceeds *via* CO intermediate over the developed catalyst.

802 | *React. Chem. Eng.*, 2022, **7**, 795–812

This journal is © The Royal Society of Chemistry 2022

Park et al.[143] studied the CO_2 hydrogenation to formic acid over heterogenised ruthenium catalysts using a fixed bed reactor with separation units. The results showed that the Ru/bpyTN-30-CTF catalyst prepared using the bpyTN-30-CTF support exhibits adequate catalytic activity for commercialisation. Under the continuous process, the catalyst displays considerable catalytic performance with the highest productivity of 669.0 g_{form}. g_{cat}^{-1} d^{-1} with CO_2 conversion of 44.8% for a superficial gas velocity of 72 cm s^{-1}. In addition, the catalyst shows excellent stability in the continuous hydrogenation process with a trickle-bed reactor over 30 days of operation, reaching a maximum turnover number of 524 000 devoid of any significant deactivation.

Bibi et al.[144] studied the hydrogenation of CO_2 using magnetic nanoparticles in a fixed bed reactor. The results showed that high activity and selectivity were obtained at 493 K, when $MnFe_2O_4$ was calcined at 513 K (0.5 °C min^{-1}) for 4 h and reduced at 553 K for 2 h, while in the case of Bi–$MnFe_2O_4$, calcination was performed at 753 K (0.5 °C min^{-1}) for 6 h and reduced at 553 K for 2 h. It was concluded that a finger-projected fixed-bed reactor in combination with magnetic nanoparticles is a highly promising alternative for industrial conversion of CO_2 to MeOH to alleviate the effects of greenhouse gases.

Microreactors for CO_2 hydrogenation

Microreactors have been widely used to generate synthetic gases and liquid fuels from direct CO_2 hydrogenation, supported by reverse water gas shift reaction and Fischer–Tropsch (FT) process, in order to produce methane, methanol, ethanol, DME and hydrocarbons. The desirable characteristics of microreactors in the field of energy technology has attracted great attention in recent years. The benefits of microreactors, such as enhanced mass and heat transfer, shorter residence time and lower pressure drops, make microreactors an interesting option for gas conversion processes in which conversion and selectivity are closely linked to the mass and heat transfer properties of the reactor and catalyst.[145] In this section, the hydrogenation of CO_2 in packed bed and membrane microreactors, as well as microwave and microplasma reactors. Fig. 8 shows a schematic representation of the membrane and microplasma reactors.

Packed bed microreactors

In packed bed microreactors, the heterogeneous catalyst is packed in a specific form into a microchannel. A packed bed microreactor provides easy loading and replacement of the catalyst.[146] Farsi et al.[147] employed a microstructured packed bed reactor (shown in Fig. 9) with internal cross-flow cooling channel to investigate the kinetics of CO_2 hydrogenation to methane by applying a 17% wt $Ni_3Fe/\gamma Al_2O_3$. The shorter bed length offered shorter contact time and prevented higher pressure drops. The results showed that the catalyst operated for over 120 min and under reaction conditions of 2 to 18 bar and 300–450 °C, CO_2 conversion to CH_4 up to 92% and methane selectivity up to 99% was achieved. Kreitz et al.[148] used a microstructured fixed bed reactor to produce methane, consisting of a 2 mm square channel. Spherical catalyst particles of 0.4 mm diameter were used to control the pressure drop and catalyst inventory. The results showed that under reaction conditions of pressure 8 bar and temperature 280 °C, a high CO_2 conversion of 97.8% was accomplished.

Belimov et al.[149] used a microstructured packed bed reactor for methanation process of CO/CO_2 mixtures by applying a commercial Ni-based catalyst to enhance the process. The results showed that after 2 h of the reaction and under conditions of 200 °C to 900 °C, CO_2 conversion up to 95% and CH_4 selectivity up to 97% was achieved.

The hydrogenation of CO_2 to methanol has often been one of the most effective and economical methods of reducing the CO_2 emissions. Jiang et al.[150] studied the catalytic hydrogenation of CO_2 to methanol over Pd/In_2O_3/
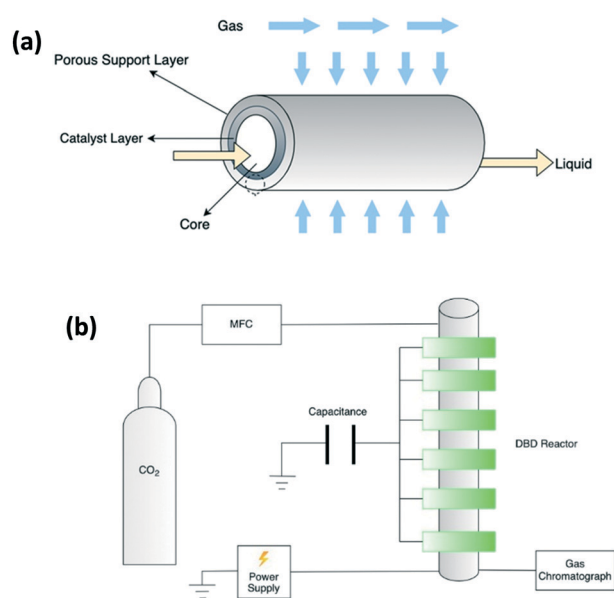

Fig. 8 Schematic representation of (a) membrane microreactor; and (b) microwave reactor set-up.
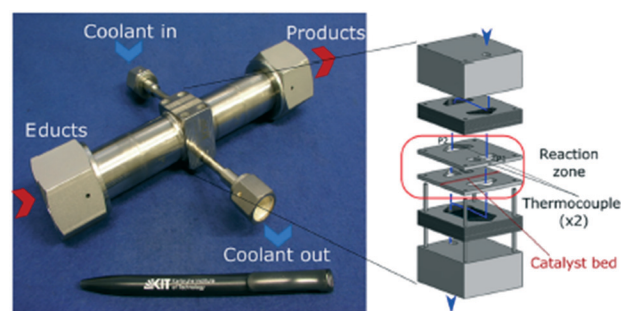

Fig. 9 Micro-structured packed-bed reactor[147] (copyright permission obtained from Elsevier).

This journal is © The Royal Society of Chemistry 2022

React. Chem. Eng., 2022, 7, 795–812 | 803

SBA-15 catalysts in a packed bed microreactor. It was found that the Pd/In$_2$O$_3$/SBA-15 catalysts exhibited superior catalytic activity with 83.9% methanol selectivity and 12.6% CO$_2$ conversion, corresponding to a STY of 1.1 × 10^{-2} mol h^{-1} g$_{cat}$$^{-1}$ under reaction conditions of 260 °C, 5 MPa and 15 000 cm^3 h^{-1} g$_{cat}$$^{-1}$. Moreover, the authors found no apparent deactivation of the catalyst during the 120 h on stream, which implies a promising industrial application of the CO$_2$ hydrogenation for methanol synthesis.

Fang et al.[151] developed a hybrid catalyst/adsorbent consisting of Cu–ZnO–ZrO$_2$ supported on hydrotalcite (named CZZ@HT) and performed the hydrogenation studies in a packed bed microreactor. The experimental results obtained using the packed bed microreactor demonstrated a methanol selectivity of 83.4% and a S_{MeOH}/S_{CO} ratio of 5 in products. A control experiment was performed by substituting the hydrotalcite in the previous catalyst, with quartz. It was revealed that significantly lower conversions at low pressures were observed for the quartz catalyst, thus depicting the desirable effect of the hydrotalcite support. Although the Cu–ZnO–ZrO$_2$ content in both catalysts was similar, the Cu surface area of the quartz catalyst was 22.7 m^2 g$_{catalyst}$$^{-1}$, as opposed to 48.2 m^2 g$_{catalyst}$$^{-1}$ for the hydrotalcite catalyst. As a result, developed hydrotalcite catalyst could achieve the same methanol productivity as the control catalyst at 2.45 MPa which is a lower reaction pressure. This lower pressure corresponds to approximately 61.3% savings in energy consumption for compression.

Koh et al.[152] investigated the structure–activity relationships of transition metal (Cr, Mn, Fe, Co, Ni) promoted copper-catalyst in direct CO$_2$ hydrogenation to methanol. The catalytic tests were performed in a continuous flow packed bed microreactor under kinetic controlled conditions. The results showed that at a reaction temperature of 180 °C, under reaction pressure of 4.0 MPa, WHSV of 60 L g$_{cat}$$^{-1}$ h^{-1}, and H$_2$:CO$_2$ mole ratio of 3:1, the catalyst presented the highest methanol yield of 10.4%. The CO$_2$ conversion achieved was 10.5% and the methanol selectivity was 98.6%.

Koh et al.[153] synthesised a series copper-catalysts, Cu–ZnO–MnO (CZM), supported on morphologically distinct siliceous porous carriers (SBA-15, MCF, KIT-6) for the direct CO$_2$ hydrogenation to methanol. The catalytic tests were performed in a packed bed microreactor. The results showed that the KIT-6 supported catalyst (CZM/KIT-6) offered the most superior performance, this is due to the morphology of KIT-6 deterred mesopore plugging, favouring the formation of small copper crystallites. Furthermore, CZM/KIT-6 retained the greatest resistance to copper crystallite growth and loss of copper surface area during reaction due to the pore-confining effect of the porous carrier and the larger inter-crystallites spacing among copper crystallites. These advantageous catalytic properties provided the highest CO$_2$ conversion (8.2%) and highest methanol production rate (105.3 mol kg$_{cat.}$$^{-1}$ h^{-1}) at low reaction temperature (180 °C). The methanol selectivity attained was ≥99% in all the experiments.

Liang et al.[145] investigated the hydrogenation of CO$_2$ to methanol using a Cu–Zn/Al foam monolithic catalyst in a packed bed microreactor. The reaction conditions used were 3 MPa and 250 °C at a high WHSV of 20 000 mL g$_{cat}$$^{-1}$ h^{-1}. The results showed that the monolith catalyst generated a high methanol yield of 7.81 g g$_{Cu}$$^{-1}$ h^{-1} and a 9.9% CO$_2$ conversion with a methanol selectivity of 82.7%. In addition, the porous aluminium pore substrate demonstrated a superior heat conductivity, and the monolithic catalyst does not change the nature of the reaction and maintains a uniform temperature distribution preventing hot spot formation.

The hydrogenation of CO$_2$ into methanol is an exothermic reaction and according to thermodynamics high pressure and lower temperature is beneficial to achieve high conversion of CO$_2$ into methanol. Typical CO$_2$ hydrogenation pressures are up to 10 MPa. Bansode et al.[95] exploited the advantages of high pressure for this reaction by performing the reactions up to 36 MPa in a microreactor to obtain almost complete conversion of CO$_2$ into methanol. Moreover, they also investigated the oxidation state of Cu in active catalyst under pressure of 20 MPa in a specially designed capillary microreactor. It was found that the Cu always remained in metallic state under the employed conditions of pressure and temperature.[154] In addition, the performance of such capillary microreactor was also elucidated and compared with conventional reactor system. As it can be seen in Fig. 10, almost identical catalytic activity was achieved in both reactors, detailing the advantage of capillary microreactor to use in situ/operando techniques which normally not possible with conventional systems.

Tidona et al.[155] employed even higher pressures of 95 MPa in stainless steel microreactor. The study shown that the compression of CO$_2$ and H$_2$ accounts only for 26% of the total energy consumption whereas the main cost was
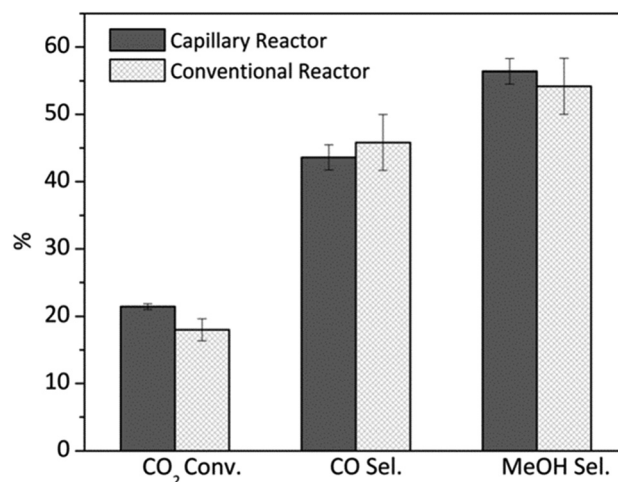

Fig. 10 Catalytic performance in terms of CO$_2$ conversion and selectivity to CO and methanol (MeOH) in CO$_2$ hydrogenation using the capillary reactor and conventional microreactor[154] (copyright permission obtained from AIP).

804 | React. Chem. Eng., 2022, **7**, 795–812

This journal is © The Royal Society of Chemistry 2022

associated with the hydrogen. This increase in pressure enhanced the space time yield by 15 times compared to literature reports.

Although packed bed microreactors have proved valuable for the hydrogenation of CO_2, these reactors can suffer from high pressure drops when using small catalyst pellets. Furthermore, the use of solid catalyst particles can lead to plugging or fowling of the microchannels, leading to the obstruction of the continuous flow. To mitigate these effects, catalytically active metals can be used to cover the inside walls of the microreactor or can be placed on poles in the reactor channels, as seen in slug flow microreactors and coated wall microreactors.[18] Furthermore, additional separation units are required to remove the desired product. Membrane microreactors offer a promising alternative due to the combination of reaction and separation zones into a single unit.[156,157]

Membrane microreactors

A membrane microreactor combines the benefits of the microreactor and the membrane reactor, this leads to better intensified processes. The membrane microreactor is able to operate under milder reaction conditions because of higher mass and heat transfer and requires lower catalyst quantities when compared to other conventional reactors.[158] Koybasi et al.[159] investigated the hydrogenation of CO_2 to DME in a membrane microreactor (Fig. 11). The reactor is comprised of identical permeate and catalyst coated reaction channels, separated by an α-Al_2O_3 supported water-selective sodalite (SOD) membrane layer. The results showed that implementing the SOD membrane layer enhanced the CO_2 conversion from 7.2% to 12.4% and increased the DME yield from 12.7% to 15.3%. The reaction conditions used to achieve this were a pressure of 50 bar, temperature 523 K, a CO_2/CO_x ratio of 0.5 and a H_2/CO_x ratio of 2. Furthermore, increasing the temperature and pressure was found to enhance the production of DME. The performance of the membrane was heavily influenced by a CO_2/CO_x ratio in the range of 0.2–0.7. Lower ratios of 0.2 promoted the undesirable production of CO_2 due to the reverse reaction. Increasing the inlet velocity of the syngas to the permeate channel promotes the membrane steam efflux and enhances the CO_2 conversion and DME yield.
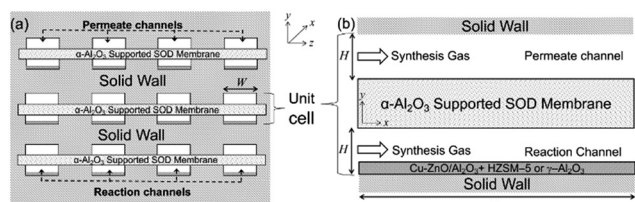

Fig. 11 Schematic representation of (a) membrane microreactor used for the hydrogenation of CO_2, and (b) combination of the channels and the membrane layer depicted as the unit cell[159] (copyright permission obtained from Elsevier).

Wang et al.[160] studied the hydrogenation of CO_2 to methanol using ZnO/t-ZrO_2 (ZrO_2 tetragonal phase) composite oxides in a membrane separation microreactor. The reaction conditions were a temperature of 320 °C, pressure 3 MPa, GHSV = 12 000 ml g^{-1} h^{-1} and a H_2/CO_2 ratio of 3 : 1. It was found that different catalyst preparation techniques substantially altered the phase structure properties of the Zn/Zr hybrid interfaces and the CO_2 hydrogenation to methanol reaction. The microreaction synthesis technique had superior technical advantages due to the unique properties of the microchannels, such as an enhanced mixing efficiency and improved mass and heat transfer. The results showed that the solid solution produced from the microreaction demonstrated a superior catalyst performance, temperature stability and catalyst regeneration perform. This was because of a highly constant solid solution structure, and rich oxygen vacancy defects. It was found that the CO_2 conversion, CH_3OH selectivity, and methanol space–time yield were 9.2%, 93.1%, and 0.35 g_{MeOH} $h^{-1}g_{cat}^{-1}$, respectively.

Despite the advantages membrane microreactors have offered for the hydrogenation of CO_2, there are limitations which exist for this technology. For example, any alterations in the surface chemical and physical properties can influence the performance of the system which directly affects the surface tension, adsorption and electro-osmosis features substantially. Moreover, small particles in the fluid zone can cause blocking of the microchannels in the reactor.[161] Microplasma reactors have become increasingly attractive due to their reduced power requirements, portability, and diminished power requirements. Furthermore, microplasmas provide a solution to the catalytic issues observed with the previously mentioned microreactors.[162]

Microwave and microplasma reactors

The application of microwave technology in chemical processes is regarded well established in organic synthesis and materials processing. Microwave reactors can be efficient in CO_2 hydrogenation to value-added chemical fuels, using heterogeneous catalysts. Reactor design plays a major role both in modelling and fabrication in microwave technology.[163]

de la Fuente et al.[164] employed a non-equilibrium microwave plasma reactor for the reduction of CO_2 with H_2. CO_2 hydrogenation was investigated in a non-thermal microwave discharge. A soli-state microwave generator with power of 200 W was applied to enhance the microwave energy to the plasma reactor. Plasma performed under pressure 7 to 200 mbar, while most of the reactants operated at pressure between 20 and 30 mbar. The results showed high CO_2 conversion to value-added chemical fuels up to 82%. Innovative microwave technology could be performed in order to define both conversion and selectivity for reactants and products under efficient control of temperature and pressure conditions.[165]

Chen *et al.*[166] studied the CO_2 hydrogenation in a microwave plasma reactor. The pulsed microwave plasma generation discharge took place in a quartz tube. An oil coolant is passed between the inner and outer tube. The results showed that the CO_2 conversion is significantly enhanced when the Ar plasma activated NiO/TiO_2 catalyst has an NiO content is approximately 10 wt%. Furthermore, the total CO_2 conversion fell from 23% to 14% for the pure CO_2 dissociation for a $H_2:CO_2$ mixture ratio of 1:9. This was due to the presence of hydrogen lowering the temperature of the electrons and diminishing the vibrational effects of CO_2. The hydrogenation of CO_2, which occurred in a non-equilibrium microwave plasma reactor, reached a total CO_2 conversion of 85% with an energy efficiency of approximately 6% and a CO_2 selectivity of 100%.

Wang *et al.*[167] performed the decomposition of pure CO_2 into CO and O_2 in a segmented electrode dielectric barrier discharge (DBD) microplasma reactor at ambient pressure. The results showed that a relatively higher CO_2 conversion and energy efficiency could be obtained at the propitious condition of longer interval between adjacent electrodes and smaller barrier thickness, and the highest CO_2 conversion and corresponding energy efficiencies are 16.9% and 3.6%, respectively, at the condition of an applied voltage of 18 kV and 1 mm barrier thickness. Furthermore, longer electrode intervals can lead to an increase in plasma density, as well as an enhanced fringe effect. Nonetheless, a smaller barrier thickness results in a smaller corresponding gas breakdown voltage, thus allowing more electrical power to be used for gas excitation. Therefore, more energetic electrons were generated and more collisions between the electrons and CO_2 molecules occurred. These factors are the main reasons for the enhanced CO_2 decomposition process.

Despite the promising applications of microplasma technology, there are some challenges which need to be overcome. Currently, the research is novel and limited. The technology suffers with issues in regard to system efficiencies, device lifetime and plasma consistencies. These plasma microreactors have experienced irregularities in plasma volume, power requirements, plasma stability, and plasma size and volume.[162]

Limitations between conventional units and microreactors

Over the past decades, great progress has been made in conventional and microreactor technology, especially on the generation of value chemical fuels through CO_2 hydrogenation. One major question now rises whether microreactors can either complete with or replace conventional units in production procedures. To respond to this question, limitations between conventional units and microreactors will be described.[168] Table 2 provides a summary of the performance of both conventional reactors and microreactors.

A continuously stirred tank reactor performs in a dynamic state, which has some difficulties to control. This condition occurs when the values of the variables in a procedure are changing over time.[169] In fluidised bed reactors, due to high mechanical load resulting from fluidisation, attrition procedures occur in relation to the catalyst and the wall of the reactor. Consequently, the catalyst deactivates. Another major limitation can be the incomplete conversion caused by bubbling. A fluidised bed reactor is restricted by external gas velocity in the reactor, however, not too low to assure minimum fluidization, and not too high in order to prevent catalyst elutriation.[170–172]

Fixed bed reactors are subject to high pressure drops. Moreover, these reactors tend to be more complex, while they exhibit higher costs.[173] Multiple fixed-bed reactors in parallel are demanded for larger plants. Preventing high pressure in the reactor tube, large-scale catalyst particles are required, resulting in lower effectiveness factors (lower catalyst activity per unit mass, resulting from difficulties of reactants to scatter in the core of the catalyst particle). Another major limitation fixed-bed reactors face is lower heat transfer from the catalyst bed and the variation of temperature into the tubes. This factor results in a) difficulty in controlling the product composition, b) hot spots in the catalyst bed that may be led to both catalyst sintering and reactor instability, and c) lower conversions of 35–40% to prevent high temperatures (in that case unreacted feed can be recycled).[174]

Table 2 Summary of the advantages and disadvantages of microreactors and conventional reactors

	Microreactors	Conventional reactors
Mass and heat transfer	Often exhibit higher mass and heat transfer due to their characteristically smaller size	Can sometimes suffer from mass and heat transfer resistances due to their larger size
Pressure drops	Pressure drops are minimal in microreactor systems	Higher pressure drops in larger packed bed reactors
Production output	The numbering up of microreactors to increase their productivity to replace industrial reactors is currently limited	The larger size of these reactors enables a larger production output for many chemical processes
Environmentally friendly	The reaction conditions for some chemical processes in microreactors are milder (*i.e.*, lower temperatures and pressures), making the processes more sustainable	The reaction conditions for the same processer are significantly higher, leading to a higher use of energy from fossil fuels
Cost	Microreactors can sometimes be associated with high fabrication costs, and the numbering up of these devices can be expensive	Conventional reactors are well established, so the construction of these units is cheaper
Residence time	The small size of the microchannels significantly reduces the residence time, achieving high conversions with shorter times	Some conventional reactors suffer from substantially longer residence times

806 | *React. Chem. Eng.*, 2022, **7**, 795–812

This journal is © The Royal Society of Chemistry 2022

Microreaction technology is considered a field that has gained significant attention due to its great performance in operation processes compared to conventional units. Microreactors offer efficient manipulation of reactions, great response time, accurate control of environmental conditions, reduced consumption of both reagents and catalysts and also provide the opportunity of an integrated instrumentation, an in-line optimisation and automation methods.[175] However, microreactors exhibit major limitations, occurred by imperfections of microreaction technology during chemical processes. Highly fabrication cost, incompatibility over solids and high economics of scaling up has led to inadequate industrial acceptance. Moreover, microreactors perform with shorter residence times, requiring the achievement of fast reactions. Fast reactions demand highly active catalysts, which should be stable in the microreactor. Consequently, microreactors cannot be applied as a replacement for classical processes yet.[176]

The comparison between conventional units and microreactors shows that higher heat and mass transfer can be accomplished by using a microreactor instead of a conventional unit, which exhibits lower bed hydrodynamics and temperature control. This characteristic is the main advantage for high exothermic reactions due to the great need of the reaction heat removal at a point where it is generated, resulting in a determined temperature profile over the reaction pathway. In addition, mixing can also be enhanced over a microreactor because of the reduced diffusion of mixing time to milliseconds.[27] Moreover, automated micro platforms have been reported in enabling design of experiments for optimization of operations conditions and reaction kinetics definition.[177] Microreactors system consisted of in-line and feedback control has been applied for the precision of operating conditions that can enhance a function for a reaction. It is significant to note that differences between microreactors and conventional units pose great challenges which require alternative prospects in order to be resolved.[175]

Future perspectives in CO_2 hydrogenation

The hydrogenation of CO_2 is considered a sustainable procedure and a promising alternative for CO_2 utilisation. However, CO_2 is regarded chemically stable and thermodynamically unfavourable. High reaction heat, different types of reactors design and sensitive catalysts, indicates CO_2 hydrogenation to value-added chemical fuels (methane, methanol, ethanol, DME and higher hydrocarbons) a challenging procedure for further research and development.

For methane generation, catalysts containing noble metals such as Ru, Rd, Rh and Ir supported by TiO_2, SiO_2, Al_2O_3 exhibit high CH_4 selectivity up to 100%, as regarded the most active metals. Ni-based catalysts such as $Ni/Ce_{0.72}Zr_{0.28}O_2$ (ref. 178) and Ni/MCM-41 (ref. 179) represent high CH_4

selectivity up to 99% and 96%, respectively. One of the crucial problems in Ni-based catalysts is considered the deactivation of the catalyst at low temperatures due the interaction of metal particles with CO and formation of nickel subcarbonyls.[4] Consequently, this problem highlights the need for process optimisation in this field.

For methanol production, catalysts consisting of Cu represent a major role in improving methanol synthesis through hydrogenation of CO_2, with the most active catalyst component supported by ZnO, ZrO_2, CeO_2, Al_2O_3 and SiO_2.[180,181] A $Cu/ZnO/Al_2O_3$ catalyst exhibits high CH_3OH selectivity up to 98%.[182] However, the bifunctional catalyst system poses major challenges for the application of a Cu/ZnO-based catalyst. Cu is considered a thermally unstable component and the size of Cu crystallites can be increased at high temperatures, resulting in the loss of the active surface and Cu sintering.[73] Furthermore, Cu-based catalysts can be poisoned, and a lower lifetime may be occurred.[183] Consequently, this challenge should emphasise the need for further research, as well as catalyst regeneration.

For ethanol synthesis, noble metal-based catalysts such as Ru and Pd supported by TiO_2, CeO_2, SiO_2 and zeolite exhibit high C_2O_5OH selectivity. A Pd/CeO_2 catalyst shows high C_2O_5OH selectivity up to 99.2%.[102] However, Mo-based and Co-based catalysts represent lower C_2O_5OH selectivity up to 10%.[184] Consequently, much research is demanded to enhance the performance of these catalysts in terms of C_2O_5OH selectivity.

For DME synthesis, a $Cu/ZnO/Al_2O_3$ catalyst shows a DME selectivity of up to 55%.[77] However, direct synthesis of DME through hydrogenation of CO_2 poses great challenges, highlighting the need for long-terms perspectives including the design of multifunctional catalyst for the interaction between methanol synthesis and methanol dehydration, enhancement of catalytic activity so as to develop an efficient product, extension of the catalyst lifetime and finally the resistance of Cu in oxidation and sintering.[185]

For higher hydrocarbons synthesis, Fe-based bimetallic catalysts supported by monometallic catalysts such as Co, Ni, Cu and Pd exhibit highly HC selectivity up to 100%.[186] Fe-silica catalysts has shown lower activity with selectivity mainly to CH_4, as the addition of the promoters can increase lower olefin selectivity up to 40%. Consequently, a more detailed understanding of both kinetics and mass transfer limitations of this procedure is demanded so as to optimize the catalysts performance.[187]

Much effort has also been dedicated to identifying the most efficient and appropriate reactor for CO_2 hydrogenation process, by comparing experimental data of different reactor types including conventional units and microreactors. The most influential factor on CO_2 hydrogenation to value-added chemical fuels is considered the reactor configuration, as different catalyst types and operating conditions are regarded most significant on product conversion and selectivity.

A fixed-bed reactor can be fabricated in either annular, or spherical configuration. A spherical fixed-bed reactor can be

This journal is © The Royal Society of Chemistry 2022

React. Chem. Eng., 2022, **7**, 795–812 | **807**

regarded as a promising alternative design compared to spherical fixed bed reactor performing under low pressure drops.[11,188,189] Another attractive alternative to enhance CO_2 hydrogenation is utilising a fluidised bed reactor, as opposed to a fixed-bed reactor. Fluidised bed reactors exhibit high heat ability and specific temperature control. Furthermore, fluidised bed reactors are regarded particularly attractive due to their potential of high exothermic reactions performing.[6]

One of the most promising alternatives for CO_2 hydrogenation to value-added chemical products is using microreactors. The necessity of microreactor technology and process performing over the last decade has proven major, especially in accelerating catalyst activity. Consequently, conventional types of reactors can be replaced by efficient and flexible micro-scale reactors.

Microwave reactors are regarded as a promising alternative for CO_2 hydrogenation to value-added chemical fuels.[164] However, a deeper understanding of microwave-assisted catalytic reactions is required to overcome complexities, limited availabilities on dielectric properties of the catalysts and major difficulties in temperature measurements.[190]

Conclusions

This review has investigated the hydrogenation of CO_2 to fuels in a range of reactors. The utilisation of CO_2 to several fuels and value-added chemical provides an attractive alternative to fossil fuels consumption. CO_2 hydrogenation to value-added chemicals and fuels is considered a promising alternative to reduce greenhouse effect. The contribution of conventional units has gained great interest due to their potential to generate methane, methanol, ethanol, DME and hydrocarbons in industrial scale. Many of the value-added chemicals produced from this process can be utilised as gas and liquid fuels for transportation, as well as important feedstocks for several other chemical industries. Although the CO_2 hydrogenation process has been investigated thoroughly in conventional reactors, such as CSTRs and FBRs, microreactors offer the opportunity to enhance the current process. Microreactors can offer higher mass and heat transfer, shorter residence times and higher CO_2 conversions. Packed bed microreactors have been used for the production of hydrocarbons and methanol from CO_2. A higher intensified process can be achieved by combining the benefits of a membrane with the advantageous properties of a microreactor. The membrane microreactor can perform the hydrogenation reaction under milder conditions because of higher mass and heat transfer and requires lower catalyst quantities when compared to other conventional macroscopic reactors. Microwave and microplasma reactors offer a more novel approach to the traditional reactors discussed in this study. These microreactors can operate at significantly milder reaction conditions, as well as higher CO_2 conversions. Future research can be directed towards investigating the hydrogenation of CO_2 for the production of a variety of fuels

and chemicals. In addition, other microreactor configurations could be explored to understand and enhance the heterogeneous chemical reaction. This further research could make the replacement of conventional reactors with microreactors viable in the future. Lastly, further research should investigate the scalability of these microreactors to produce fuels on an industrial scale.

Nomenclature

CCS	Carbon capture and storage
CCU	Carbon capture and utilization
CSTR	Continuously stirred tank reactor
CO_2	Carbon dioxide
H_2	Hydrogen
CH_4 (C_1)	Methane
CH_2OH	Methanol
C_2H_2OH	Ethanol
DME	Dimethyl ether
FT	Fischer–Tropsch
RWGS	Reverse water gas reaction
Ni	Nickel
Cu	Copper
Mo	Molybdenum
Co	Cobalt
Li	Lithium
Na	Sodium
K	Potassium
Mn	Manganese
Fe	Iron
Ce	Cerium
Rh	Rhodium
Ir	Iridium
Pt	Platinum
Ru	Ruthenium
In	Indium
Pd	Palladium
CeO_2	Cerium oxide
MnO_2	Manganese oxide
In_2O_3	Indium oxide
NiO	Nickel
TiO_2	Titanium oxide
SiO_2	Silicon dioxide
Fe_2O_3	Iron oxide
K_2CO_3	Potassium carbonate
NiCo	Catalyst
ZnO	Zinc oxide
Co_3O_4	Cerium oxide
ZrO_2	Zirconium oxide
PdZn	Catalyst
SBA-15	Mesoporous silica catalyst
ZrO_2	Zirconium dioxide
γ-Al_2O_3	Gamma-alumina
P	Pressure (bar)
T	Temperature (°C)
H_2O	Water

808 | React. Chem. Eng., 2022, 7, 795–812

This journal is © The Royal Society of Chemistry 2022

s	Second
h	Hour
K	Kelvin
mL	Milliliter
m	Meter
μm	Micro-meter
mm	Millimeter
cm³	Cubic centimeter
min	Minute
DBT	Dibenzyltoluene
NPs	Nanoparticles
Gt	Gigatons

Conflicts of interest

There are no conflicts to declare.

Acknowledgements

References

1 M. Bui, C. S. Adjiman, A. Bardow, E. J. Anthony, A. Boston, S. Brown, P. S. Fennell, S. Fuss, A. Galindo, L. A. Hackett, J. P. Hallett, H. J. Herzog, G. Jackson, J. Kemper, S. Krevor, G. C. Maitland, M. Matuszewski, I. S. Metcalfe, C. Petit, G. Puxty, J. Reimer, D. M. Reiner, E. S. Rubin, S. A. Scott, N. Shah, B. Smit, J. P. M. Trusler, P. Webley, J. Wilcox and N. Mac Dowell, *Energy Environ. Sci.*, 2018, **11**, 1062–1176.

2 D. Gielen, F. Boshell, D. Saygin, M. D. Bazilian, N. Wagner and R. Gorini, *Energy Strategy Rev.*, 2019, **24**, 38–50.

3 X. Xiaoding and J. Moulijn, *Energy Fuels*, 1996, **10**, 305–325.

4 W. Wang, S. Wang, X. Ma and J. Gong, *Chem. Soc. Rev.*, 2011, **40**, 3703–3727.

5 H. Nieminen, A. Laari and T. Koiranen, *Processes*, 2019, **7**, 405.

6 S. Saeidi, S. Najari, V. Hessel, K. Wilson, F. J. Keil, P. Concepción, S. L. Suib and A. E. Rodrigues, *Prog. Energy Combust. Sci.*, 2021, **85**, 100905.

7 R. Lindsey, *Climate Change: Atmospheric Carbon Dioxide*, https://www.climate.gov/news-features/understanding-climate/climate-change-atmospheric-carbon-dioxide, 2020.

8 F. M. Baena-Moreno, M. Rodríguez-Galán, F. Vega, B. Alonso-Fariñas, L. F. Vilches Arenas and B. Navarrete, *Energy Sources, Part A*, 2018, **41**, 1403–1433.

9 D. Carrales-Alvarado, A. Dongil, J. Fernández-Morales, M. Fernández-García, A. Guerrero-Ruiz and I. Rodríguez-Ramos, *Catal. Sci. Technol.*, 2020, **10**, 6790–6799.

10 Z. Zhang, S.-Y. Pan, H. Li, J. Cai, A. G. Olabi, E. J. Anthony and V. Manovic, *Renewable Sustainable Energy Rev.*, 2020, **125**, 109799.

11 D. Iranshahi, A. Golrokh, E. Pourazadi, S. Saeidi and F. Gallucci, *Chem. Eng. Process.*, 2018, **132**, 16–24.

12 G. Zsembinszki, A. Solé, C. Barreneche, C. Prieto, A. Fernández and L. Cabeza, *Energies*, 2018, **11**, 2358.

13 A. Solé, I. Martorell and L. F. Cabeza, *Renewable Sustainable Energy Rev.*, 2015, **47**, 386–398.

14 W. K. Fan and M. Tahir, *Chem. Eng. J.*, 2022, **427**, 131617.

15 M. Ronda-Lloret, Y. Wang, P. Oulego, G. Rothenberg, X. Tu and N. R. Shiju, *ACS Sustainable Chem. Eng.*, 2020, **8**, 17397–17407.

16 S. B. Jo, J. H. Woo, J. H. Lee, T. Y. Kim, H. I. Kang, S. C. Lee and J. C. Kim, *Sustainable Energy Fuels*, 2020, **4**, 4679–4687.

17 Z. Ma and M. D. Porosoff, *ACS Catal.*, 2019, **9**, 2639–2656.

18 S. Hafeez, G. Manos, S. M. Al-Salem, E. Aristodemou and A. Constantinou, *React. Chem. Eng.*, 2018, **3**, 414–432.

19 X. Yao, Y. Zhang, L. Du, J. Liu and J. Yao, *Renewable Sustainable Energy Rev.*, 2015, **47**, 519–539.

20 S. Hafeez, E. Aristodemou, G. Manos, S. M. Al-Salem and A. Constantinou, *RSC Adv.*, 2020, **10**, 41680–41692.

21 G. Wu, E. Cao, P. Ellis, A. Constantinou, S. Kuhn and A. Gavriilidis, *Chem. Eng. Sci.*, 2019, **201**, 386–396.

22 S. Hafeez, E. Aristodemou, G. Manos, S. Al-Salem and A. Constantinou, *React. Chem. Eng.*, 2020, **5**, 1083–1092.

23 S. Hafeez, F. Sanchez, S. M. Al-Salem, A. Villa, G. Manos, N. Dimitratos and A. Constantinou, *Catalysts*, 2021, **11**, 341.

24 G. Wu, E. Cao, P. Ellis, A. Constantinou, S. Kuhn and A. Gavriilidis, *Chem. Eng. J.*, 2019, **377**, 120086.

25 A. Constantinou, G. Wu, B. Venezia, P. Ellis, S. Kuhn and A. Gavriilidis, *Top. Catal.*, 2019, **62**, 1126–1131.

26 A. A. Bojang and H.-S. Wu, *Processes*, 2020, **8**, 891.

27 T. Illg, P. Lob and V. Hessel, *Bioorg. Med. Chem.*, 2010, **18**, 3707–3719.

28 A. Tanimu, S. Jaenicke and K. Alhooshani, *Chem. Eng. J.*, 2017, **327**, 792–821.

29 D. L. Trimm, *Catal. Today*, 1997, **37**, 233–238.

30 J. Dufour, D. P. Serrano, J. L. Gálvez, J. Moreno and A. González, *Energy Fuels*, 2011, **25**, 2194–2202.

31 S. Lin, M. Harada, Y. Suzuki and H. Hatano, *Fuel*, 2002, **81**, 2079–2085.

32 A. Bisio and S. Boots, *Encyclopedia of energy technology and the environment*, Wiley, 1995.

33 S. S. Kumar and V. Himabindu, *Mater. Sci. Energy Technol.*, 2019, **2**, 442–454.

34 J. Chi and H. Yu, *Chin. J. Catal.*, 2018, **39**, 390–394.

35 G. Liu, Y. Sheng, J. W. Ager, M. Kraft and R. Xu, *EnergyChem*, 2019, **1**, 100014.

36 S. Saeidi, N. A. S. Amin and M. R. Rahimpour, *J. CO2 Util.*, 2014, **5**, 66–81.

37 H. L. Huynh, W. M. Tucho, X. Yu and Z. Yu, *J. Cleaner Prod.*, 2020, 264.

38 A. Saravanan, P. S. Kumar, D.-V. N. Vo, S. Jeevanantham, V. Bhuvaneswari, V. A. Narayanan, P. R. Yaashikaa, S. Swetha and B. Reshma, *Chem. Eng. Sci.*, 2021, **236**, 116515.

39 P. Gao, L. Zhang, S. Li, Z. Zhou and Y. Sun, *ACS Cent. Sci.*, 2020, **6**, 1657–1670.

40 G. Zhou, H. Liu, Y. Xing, S. Xu, H. Xie and K. Xiong, *J. CO2 Util.*, 2018, **26**, 221–229.

41 J. Wang, G. Li, Z. Li, C. Tang, Z. Feng, H. An, H. Liu, T. Liu and C. Li, *Sci. Adv.*, 2017, **3**, e1701290.

42 J.-N. Zheng, A. Kang, J.-M. Wang, L. Jing and L. Yuan, *J. Fuel Chem. Technol.*, 2019, **47**, 697–708.

This journal is © The Royal Society of Chemistry 2022

React. Chem. Eng., 2022, **7**, 795–812 | **809**

43 C. G. Visconti, M. Martinelli, L. Falbo, A. Infantes-Molina, L. Lietti, P. Forzatti, G. Iaquaniello, E. Palo, B. Picutti and F. Brignoli, *Appl. Catal., B*, 2017, **200**, 530–542.

44 S. Rönsch, J. Schneider, S. Matthischke, M. Schlüter, M. Götz, J. Lefebvre, P. Prabhakaran and S. Bajohr, *Fuel*, 2016, **166**, 276–296.

45 S. Biswas, A. P. Kulkarni, S. Giddey and S. Bhattacharya, *Front. Energy Res.*, 2020, **8**, 229.

46 H. Cao, W. Wang, T. Cui, H. Wang, G. Zhu and X. Ren, *Energies*, 2020, **13**, 2235.

47 T. Franken, J. Terreni, A. Borgschulte and A. Heel, *J. Catal.*, 2020, **382**, 385–394.

48 F. W. Keen and M. Tahir, *J. Environ. Chem. Eng.*, 2021, 105460.

49 J. Lee, S. Kim, Y. T. Kim, G. Kwak and J. Kim, *Energy*, 2020, **199**, 117437.

50 S. Renda, A. Ricca and V. Palma, *Appl. Energy*, 2020, **279**, 115767.

51 I. S. Pieta, A. Lewalska-Graczyk, P. Kowalik, K. Antoniak-Jurak, M. Krysa, A. Sroka-Bartnicka, A. Gajek, W. Lisowski, D. Mrdenovic and P. Pieta, *Catalysts*, 2021, **11**, 433.

52 H. P. Shivaraju, K. M. Anilkumar, S. R. Yashas, R. Harini, B. Shahmoradi, A. Maleki and G. McKay, *Biofuels, Bioprod. Biorefin.*, 2021, **15**, 189–201.

53 G. Varvoutis, M. Lykaki, S. Stefa, E. Papista, S. A. Carabineiro, G. E. Marnellos and M. Konsolakis, *Catal. Commun.*, 2020, **142**, 106036.

54 J. Zhang, Y. Yang, J. Liu and B. Xiong, *Appl. Surf. Sci.*, 2021, **558**, 149866.

55 C. V. Miguel, M. A. Soria, A. Mendes and L. M. Madeira, *J. Nat. Gas Sci. Eng.*, 2015, **22**, 1–8.

56 P. J. Lunde and F. L. Kester, *Ind. Eng. Chem. Process Des. Dev.*, 1974, **13**, 27–33.

57 D. Schlereth and O. Hinrichsen, *Chem. Eng. Res. Des.*, 2014, **92**, 702–712.

58 J. Cored, A. García-Ortiz, S. Iborra, M. J. Climent, L. Liu, C.-H. Chuang, T.-S. Chan, C. Escudero, P. Concepción and A. Corma, *J. Am. Chem. Soc.*, 2019, **141**, 19304–19311.

59 P. Dongapure, S. Bagchi, S. Mayadevi and R. N. Devi, *Mol. Catal.*, 2020, **482**, 110700.

60 J. Wang, K. Sun, X. Jia and C.-J. Liu, *Catal. Today*, 2021, **365**, 341–347.

61 C. Wang, E. Guan, L. Wang, X. Chu, Z. Wu, J. Zhang, Z. Yang, Y. Jiang, L. Zhang and X. Meng, *J. Am. Chem. Soc.*, 2019, **141**, 8482–8488.

62 X. Chen, X. Su, H. Duan, B. Liang, Y. Huang and T. Zhang, *Catal. Today*, 2017, **281**, 312–318.

63 F. Hu, X. Chen, Z. Tu, Z.-H. Lu, G. Feng and R. Zhang, *Ind. Eng. Chem. Res.*, 2021, **60**, 12235–12243.

64 H. Liu, S. Xu, G. Zhou, G. Huang, S. Huang and K. Xiong, *Chem. Eng. J.*, 2018, **351**, 65–73.

65 S. Kattel, P. J. Ramírez, J. G. Chen, J. A. Rodriguez and P. Liu, *Science*, 2017, **355**, 1296–1299.

66 K. Chen, H. Fang, S. Wu, X. Liu, J. Zheng, S. Zhou, X. Duan, Y. Zhuang, S. C. E. Tsang and Y. Yuan, *Appl. Catal., B*, 2019, **251**, 119–129.

67 K.-I. Tominaga, Y. Sasaki, M. Saito, K. Hagihara and T. Watanabe, *J. Mol. Catal.*, 1994, **89**, 51–55.

68 Z. He, Q. Qian, J. Ma, Q. Meng, H. Zhou, J. Song, Z. Liu and B. Han, *Angew. Chem., Int. Ed.*, 2016, **55**, 737–741.

69 S. Zhang, X. Liu, Z. Shao, H. Wang and Y. Sun, *J. Catal.*, 2020, **382**, 86–96.

70 M. R. Gogate and R. J. Davis, *Catal. Commun.*, 2010, **11**, 901–906.

71 L. Ding, T. Shi, J. Gu, Y. Cui, Z. Zhang, C. Yang, T. Chen, M. Lin, P. Wang and N. Xue, *Chem*, 2020, **6**, 2673–2689.

72 X. Wang, P. J. Ramírez, W. Liao, J. A. Rodriguez and P. Liu, *J. Am. Chem. Soc.*, 2021, **143**, 13103–13112.

73 S. Ren, W. R. Shoemaker, X. Wang, Z. Shang, N. Klinghoffer, S. Li, M. Yu, X. He, T. A. White and X. Liang, *Fuel*, 2019, **239**, 1125–1133.

74 S. Ren, X. Fan, Z. Shang, W. R. Shoemaker, L. Ma, T. Wu, S. Li, N. B. Klinghoffer, M. Yu and X. Liang, *J. CO2 Util.*, 2020, **36**, 82–95.

75 Q. Sheng, R.-P. Ye, W. Gong, X. Shi, B. Xu, M. Argyle, H. Adidharma and M. Fan, *J. Environ. Sci.*, 2020, **92**, 106–117.

76 D. F. Carvalho, G. C. Almeida, R. S. Monteiro and C. J. Mota, *Energy Fuels*, 2020, **34**, 7269–7274.

77 H. Ham, N. T. Xuan, H. S. Jung, J. Kim, H.-S. Roh and J. W. Bae, *Catal. Today*, 2021, **369**, 112–122.

78 G. Bonura, C. Cannilla, L. Frusteri, E. Catizzone, S. Todaro, M. Migliori, G. Giordano and F. Frusteri, *Catal. Today*, 2020, **345**, 175–182.

79 G. Bonura, M. Migliori, L. Frusteri, C. Cannilla, E. Catizzone, G. Giordano and F. Frusteri, *J. CO2 Util.*, 2018, **24**, 398–406.

80 Y. Xu, P. Zhai, Y. Deng, J. Xie, X. Liu, S. Wang and D. Ma, *Angew. Chem.*, 2020, **132**, 21920–21928.

81 K. Y. Kim, H. Lee, W. Y. Noh, J. Shin, S. J. Han, S. K. Kim, K. An and J. S. Lee, *ACS Catal.*, 2020, **10**, 8660–8671.

82 T. Witoon, V. Lapkeatseree, T. Numpilai, C. K. Cheng and J. Limtrakul, *Chem. Eng. J.*, 2022, **428**, 131389.

83 S. Kattel, P. Liu and J. G. Chen, *J. Am. Chem. Soc.*, 2017, **139**, 9739–9754.

84 S. Dang, B. Qin, Y. Yang, H. Wang, J. Cai, Y. Han, S. Li, P. Gao and Y. Sun, *Sci. Adv.*, 2020, **6**, eaaz2060.

85 F. Jiang, S. Wang, B. Liu, J. Liu, L. Wang, Y. Xiao, Y. Xu and X. Liu, *ACS Catal.*, 2020, **10**, 11493–11509.

86 X. Jiang, X. Nie, Y. Gong, C. M. Moran, J. Wang, J. Zhu, H. Chang, X. Guo, K. S. Walton and C. Song, *J. Catal.*, 2020, **383**, 283–296.

87 N. Rui, K. Sun, C. Shen and C.-J. Liu, *J. CO2 Util.*, 2020, **42**, 101313.

88 J. Song, S. Liu, C. Yang, G. Wang, H. Tian, Z.-J. Zhao, R. Mu and J. Gong, *Appl. Catal., A*, 2020, **263**, 118367.

89 J. Wang, G. Zhang, J. Zhu, X. Zhang, F. Ding, A. Zhang, X. Guo and C. Song, *ACS Catal.*, 2021, **11**, 1406–1423.

90 C. Yang, C. Pei, R. Luo, S. Liu, Y. Wang, Z. Wang, Z.-J. Zhao and J. Gong, *J. Am. Chem. Soc.*, 2020, **142**, 19523–19531.

91 J. Yu, M. Yang, J. Zhang, Q. Ge, A. Zimina, T. Pruessmann, L. Zheng, J.-D. Grunwaldt and J. Sun, *ACS Catal.*, 2020, **10**, 14694–14706.

810 | *React. Chem. Eng.*, 2022, **7**, 795–812

This journal is © The Royal Society of Chemistry 2022

92 K. M. Vanden Bussche and G. F. Froment, *J. Catal.*, 1996, **161**, 1–10.

93 W. Schakel, G. Oreggioni, B. Singh, A. Strømman and A. Ramírez, *J. CO2 Util.*, 2016, **16**, 138–149.

94 N. Rui, Z. Wang, K. Sun, J. Ye, Q. Ge and C.-J. Liu, *Appl. Catal., B*, 2017, **218**, 488–497.

95 A. Bansode and A. Urakawa, *J. Catal.*, 2014, **309**, 66–70.

96 O. Martin, A. J. Martín, C. Mondelli, S. Mitchell, T. F. Segawa, R. Hauert, C. Drouilly, D. Curulla-Ferré and J. Pérez-Ramírez, *Angew. Chem., Int. Ed.*, 2016, **55**, 6261–6265.

97 J. Zhong, X. Yang, Z. Wu, B. Liang, Y. Huang and T. Zhang, *Chem. Soc. Rev.*, 2020, **49**, 1385–1413.

98 Y. Hartadi, D. Widmann and R. J. Behm, *ChemSusChem*, 2015, **8**, 456–465.

99 A. S. Malik, S. F. Zaman, A. A. Al-Zahrani, M. A. Daous, H. Driss and L. A. Petrov, *Appl. Catal., A*, 2018, **560**, 42–53.

100 K. An, S. Zhang, J. Wang, Q. Liu, Z. Zhang and Y. Liu, *J. Energy Chem.*, 2021, **56**, 486–495.

101 A. Goryachev, A. Pustovarenko, G. Shterk, N. S. Alhajri, A. Jamal, M. Albuali, L. van Koppen, I. S. Khan, A. Russkikh and A. Ramirez, *ChemCatChem*, 2021, **13**, 3324.

102 Y. Lou, F. Jiang, W. Zhu, L. Wang, T. Yao, S. Wang, B. Yang, B. Yang, Y. Zhu and X. Liu, *Appl. Catal., B*, 2021, **291**, 120122.

103 P. Riani, G. Garbarino, T. Cavattoni and G. Busca, *Catal. Today*, 2021, **365**, 122–131.

104 X. Ye, C. Yang, X. Pan, J. Ma, Y. Zhang, Y. Ren, X. Liu, L. Li and Y. Huang, *J. Am. Chem. Soc.*, 2020, **142**, 19001–19005.

105 H. Zhang, H. Han, L. Xiao and W. Wu, *ChemCatChem*, 2021, **13**, 3333.

106 S. Zhang, Z. Wu, X. Liu, Z. Shao, L. Xia, L. Zhong, H. Wang and Y. Sun, *Appl. Catal., A*, 2021, **293**, 120207.

107 X. He, *Int. J. Oil, Gas Coal Eng.*, 2017, **5**, 145–152.

108 E. Catizzone, G. Bonura, M. Migliori, F. Frusteri and G. Giordano, *Molecules*, 2017, **23**, 31.

109 X. Fan, S. Ren, B. Jin, S. Li, M. Yu and X. Liang, *Chin. J. Chem. Eng.*, 2020, **38**, 106–113.

110 X. Fang, H. Jia, B. Zhang, Y. Li, Y. Wang, Y. Song, T. Du and L. Liu, *J. Environ. Chem. Eng.*, 2021, **9**, 105299.

111 T. T. N. Vu, A. Desgagnés and M. C. Iliuta, *Appl. Catal., A*, 2021, **617**, 118119.

112 L. Yao, X. Shen, Y. Pan and Z. Peng, *Energy Fuels*, 2020, **34**, 8635–8643.

113 G. Bonura, M. Cordaro, C. Cannilla, A. Mezzapica, L. Spadaro, F. Arena and F. Frusteri, *Catal. Today*, 2014, **228**, 51–57.

114 A. Alvarez, A. Bansode, A. Urakawa, A. V. Bavykina, T. A. Wezendonk, M. Makkee, J. Gascon and F. Kapteijn, *Chem. Rev.*, 2017, **117**, 9804–9838.

115 H. Bahruji, R. D. Armstrong, J. Ruiz Esquius, W. Jones, M. Bowker and G. J. Hutchings, *Ind. Eng. Chem. Res.*, 2018, **57**, 6821–6829.

116 K. C. Tokay, T. Dogu and G. Dogu, *Chem. Eng. J.*, 2012, **184**, 278–285.

117 S. Michailos, S. McCord, V. Sick, G. Stokes and P. Styring, *Energy Convers. Manage.*, 2019, **184**, 262–276.

118 A. Nakhaei Pour and M. R. Housaindokht, *J. Energy Chem.*, 2017, **26**, 359–367.

119 M. Albrecht, U. Rodemerck, M. Schneider, M. Bröring, D. Baabe and E. V. Kondratenko, *Appl. Catal., B*, 2017, **204**, 119–126.

120 R. Satthawong, N. Koizumi, C. Song and P. Prasassarakich, *J. CO2 Util.*, 2013, **3**, 102–106.

121 A. E. Gamboa-Torres and A. Flores-Tlacuahuac, *Chem. Eng. J.*, 2000, **77**, 153–164.

122 L. Özkan, M. V. Kothare and C. Georgakis, *Chem. Eng. Sci.*, 2003, **58**, 1207–1221.

123 D. L. Chiavassa, J. Barrandeguy, A. L. Bonivardi and M. A. Baltanás, *Catal. Today*, 2008, **133-135**, 780–786.

124 R. W. Dorner, D. R. Hardy, F. W. Williams and H. D. Willauer, *Appl. Catal., A*, 2010, **373**, 112–121.

125 J. Lefebvre, N. Trudel, S. Bajohr and T. Kolb, *Fuel*, 2018, **217**, 151–159.

126 F. Kirchbacher, P. Biegger, M. Miltner, M. Lehner and M. Harasek, *Energy*, 2018, **146**, 34–46.

127 A. García-Trenco, A. Regoutz, E. R. White, D. J. Payne, M. S. P. Shaffer and C. K. Williams, *Appl. Catal., B*, 2018, **220**, 9–18.

128 A. S. García-Trenco, E. R. White, A. Regoutz, D. J. Payne, M. S. Shaffer and C. K. Williams, *ACS Catal.*, 2017, **7**, 1186–1196.

129 M. Huš, D. Kopač, N. S. Štefančič, D. L. Jurković, V. D. Dasireddy and B. Likozar, *Catal. Sci. Technol.*, 2017, **7**, 5900–5913.

130 J.-S. Kim, S. Lee, S.-B. Lee, M.-J. Choi and K.-W. Lee, *Catal. Today*, 2006, **115**, 228–234.

131 H. Nam, J. H. Kim, H. Kim, M. J. Kim, S.-G. Jeon, G.-T. Jin, Y. Won, B. W. Hwang, S.-Y. Lee, J.-I. Baek, D. Lee, M. W. Seo and H.-J. Ryu, *Energy*, 2021, **214**, 118895.

132 C. Jia, Y. Dai, Y. Yang and J. W. Chew, *Int. J. Hydrogen Energy*, 2019, **44**, 13443–13455.

133 A. Pietschak, J. Maußner, A. G. Dixon and H. Freund, *Int. J. Heat Mass Transfer*, 2020, **148**, 119099.

134 H. D. Willauer, R. Ananth, M. T. Olsen, D. M. Drab, D. R. Hardy and F. W. Williams, *J. CO2 Util.*, 2013, **3-4**, 56–64.

135 M. Iglesias González, H. Eilers and G. Schaub, *Energy Technol.*, 2016, **4**, 90–103.

136 J. Ducamp, A. Bengaouer and P. Baurens, *Can. J. Chem. Eng.*, 2017, **95**, 241–252.

137 M. M. Jaffar, M. A. Nahil and P. T. Williams, *Energy Technol.*, 2019, **7**, 1900795.

138 L. Kiewidt and J. Thöming, *Chem. Eng. Sci.*, 2015, **132**, 59–71.

139 B. Castellani, A. Gambelli, E. Morini, B. Nastasi, A. Presciutti, M. Filipponi, A. Nicolini and F. Rossi, *Energies*, 2017, **10**, 855.

140 L. Pastor-Pérez, V. Patel, E. Le Saché and T. R. Reina, *J. Energy Inst.*, 2020, **93**, 415–424.

141 M. J. Bradley, R. Ananth, H. D. Willauer, J. W. Baldwin, D. R. Hardy, F. DiMascio and F. W. Williams, *J. CO2 Util.*, 2017, **17**, 1–9.

142 Z. Zhang, H. Yin, G. Yu, S. He, J. Kang, Z. Liu, K. Cheng, Q. Zhang and Y. Wang, *J. Catal.*, 2021, **395**, 350–361.

This journal is © The Royal Society of Chemistry 2022

React. Chem. Eng., 2022, **7**, 795–812 | 811

143 K. Park, G. H. Gunasekar, S.-H. Kim, H. Park, S. Kim, K. Park, K.-D. Jung and S. Yoon, *Green Chem.*, 2020, **22**, 1639–1649.

144 M. Bibi, R. Ullah, M. Sadiq, S. Sadiq, I. Khan, K. Saeed, M. A. Zia, Z. Iqbal, I. Ullah and Z. Iqbal, *Catalysts*, 2021, **11**, 592.

145 Z. Liang, P. Gao, Z. Tang, M. Lv and Y. Sun, *J. CO2 Util.*, 2017, **21**, 191–199.

146 A. Gavriilidis, A. Constantinou, K. Hellgardt, K. K. Hii, G. J. Hutchings, G. L. Brett, S. Kuhn and S. P. Marsden, *React. Chem. Eng.*, 2016, **1**, 595–612.

147 S. Farsi, W. Olbrich, P. Pfeifer and R. Dittmeyer, *Chem. Eng. J.*, 2020, **388**, 124233.

148 B. Kreitz, G. D. Wehinger and T. Turek, *Chem. Eng. Sci.*, 2019, **195**, 541–552.

149 M. Belimov, D. Metzger and P. Pfeifer, *AIChE J.*, 2017, **63**, 120–129.

150 H. Jiang, J. Lin, X. Wu, W. Wang, Y. Chen and M. Zhang, *J. CO2 Util.*, 2020, **36**, 33–39.

151 X. Fang, Y. Men, F. Wu, Q. Zhao, R. Singh, P. Xiao, T. Du and P. A. Webley, *Int. J. Hydrogen Energy*, 2019, **44**, 21913–21925.

152 M. K. Koh, M. M. Zain and A. R. Mohamed, *AIP Conf. Proc.*, 2019, **2124**, 020006.

153 M. K. Koh, M. Khavarian, S. P. Chai and A. R. Mohamed, *Int. J. Hydrogen Energy*, 2018, **43**, 9334–9342.

154 A. Bansode, G. Guilera, V. Cuartero, L. Simonelli, M. Avila and A. Urakawa, *Rev. Sci. Instrum.*, 2014, **85**, 084105.

155 B. Tidona, C. Koppold, A. Bansode, A. Urakawa and P. R. von Rohr, *J. Supercrit. Fluids*, 2013, **78**, 70–77.

156 S. Hafeez, S. Al-Salem and A. Constantinou, in *Membranes for Environmental Applications*, Springer, 2020, pp. 383–411.

157 S. Hafeez, S. Al-Salem, G. Manos and A. Constantinou, *Environ. Chem. Lett.*, 2020, **18**, 1477–1490.

158 X. Tan and K. Li, *J. Chem. Technol. Biotechnol.*, 2013, **88**, 1771–1779.

159 H. H. Koybasi and A. K. Avci, *Catal. Today*, 2022, **383**, 133–145.

160 X. Wang, Y. Wang, C. Yang, Y. Yi, X. Wang, F. Liu, J. Cao and H. Pan, *Appl. Catal., A*, 2020, **595**, 117507.

161 M. R. Kiani, M. Meshksar, M. A. Makarem and E. Rahimpour, *Top. Catal.*, 2021, 1–20.

162 P. J. Lindner, S. Y. Hwang and R. Besser, *Energy Fuels*, 2013, **27**, 4432–4440.

163 P. Priecel and J. A. Lopez-Sanchez, *ACS Sustainable Chem. Eng.*, 2018, **7**, 3–21.

164 J. F. de la Fuente, S. H. Moreno, A. I. Stankiewicz and G. D. Stefanidis, *Int. J. Hydrogen Energy*, 2016, **41**, 21067–21077.

165 M. B. Gawande, S. N. Shelke, R. Zboril and R. S. Varma, *Acc. Chem. Res.*, 2014, **47**, 1338–1348.

166 G. Chen, N. Britun, T. Godfroid, V. Georgieva, R. Snyders and M.-P. Delplancke-Ogletree, *J. Phys. D: Appl. Phys.*, 2017, **50**, 084001.

167 B. Wang, X. Wang and H. Su, *Plasma Chem. Plasma Process.*, 2020, **40**, 1189–1206.

168 E. R. Delsman, B. J. P. F. Laarhoven, M. H. J. M. D. Croon, G. J. Kramer and J. C. Schouten, *Chem. Eng. Res. Des.*, 2005, **83**, 1063–1075.

169 N. Abdullah, T. C. Yee, A. Mohamed, M. M. Mustafa, M. H. Osman and A. B. Mohamad, *Indian J. Sci. Technol.*, 2016, **9**, 1–7.

170 M. Götz, J. Lefebvre, F. Mörs, A. McDaniel Koch, F. Graf, S. Bajohr, R. Reimert and T. Kolb, *Renewable Energy*, 2016, **85**, 1371–1390.

171 C. H. Bartholomew, *Appl. Catal., A*, 2001, **212**, 17–60.

172 M. C. Seemann, T. J. Schildhauer and S. M. A. Biollaz, *Ind. Eng. Chem. Res.*, 2010, **49**, 7034–7038.

173 X. Zhang, W. Qian, H. Zhang, Q. Sun and W. Ying, *Chin. J. Chem. Eng.*, 2018, **26**, 245–251.

174 X. Wang and M. Economides, *Journal*, 2009, 368, DOI: 10.1016/B978-1-933762-38-8.50014-9.

175 N. Al-Rifai, E. Cao, V. Dua and A. Gavriilidis, *Curr. Opin. Chem. Eng.*, 2013, **2**, 338–345.

176 A. Šalić, A. Tušek and B. Zelić, *J. Appl. Biomed.*, 2012, **10**, 137–153.

177 M. M. E. Delville, P. J. Nieuwland, P. Janssen, K. Koch, J. C. M. van Hest and F. P. J. T. Rutjes, *Chem. Eng. J.*, 2011, **167**, 556–559.

178 F. Ocampo, B. Louis and A.-C. Roger, *Appl. Catal., A*, 2009, **369**, 90–96.

179 G. Du, S. Lim, Y. Yang, C. Wang, L. Pfefferle and G. Haller, *J. Catal.*, 2007, **249**, 370–379.

180 F. Arena, K. Barbera, G. Italiano, G. Bonura, L. Spadaro and F. Frusteri, *J. Catal.*, 2007, **249**, 185–194.

181 M. Saito and K. Murata, *Catal. Surv. Asia*, 2004, **8**, 285–294.

182 M. Behrens, F. Studt, I. Kasatkin, S. Kuhl, M. Havecker, F. Abild-Pedersen, S. Zander, F. Girgsdies, P. Kurr, B. L. Kniep, M. Tovar, R. W. Fischer, J. K. Norskov and R. Schlogl, *Science*, 2012, **336**, 893–897.

183 F. Zeng, C. Mebrahtu, X. Xi, L. Liao, J. Ren, J. Xie, H. J. Heeres and R. Palkovits, *Appl. Catal., B*, 2021, **291**, 120073.

184 S. Liu, H. Zhou, Q. Song and Z. Ma, *J. Taiwan Inst. Chem. Eng.*, 2017, **76**, 18–26.

185 G. Bonura, C. Cannilla, L. Frusteri, A. Mezzapica and F. Frusteri, *Catal. Today*, 2017, **281**, 337–344.

186 R. Satthawong, N. Koizumi, C. Song and P. Prasassarakich, *Top. Catal.*, 2013, **57**, 588–594.

187 R. E. Owen, D. Mattia, P. Plucinski and M. D. Jones, *ChemPhysChem*, 2017, **18**, 3211–3218.

188 D. Iranshahi, P. Salimi, Z. Pourmand, S. Saeidi and J. J. Klemeš, *Chem. Eng. Process.*, 2017, **120**, 258–267.

189 S. Najari, S. Saeidi, G. Gróf, F. J. Keil and A. E. Rodrigues, *Energy Convers. Manage.*, 2020, **226**, 113550.

190 Y. Deng, X. Bai, V. Abdelsayed, D. Shekhawat, P. D. Muley, S. Karpe, C. Mevawala, D. Bhattacharyya, B. Robinson, A. Caiola, J. B. Powell, A. P. van Bavel, J. Hu and G. Veser, *Chem. Eng. J.*, 2021, **420**, 129670.